Exploring Mechanomyography as a Tool for Fatigue Monitoring in Neurorehabilitation

by

Ann Ryan Johnston

A thesis submitted to the Graduate Faculty of
Auburn University
in partial fulfillment of the
requirements for the Degree of
Master of Science

Auburn, Alabama
August 9, 2025

Keywords: Mechanomyography, Biomechanical Assessment, Assistive and Rehabilitative Technologies

Approved by

Chad G. Rose, Chair, Assistant Professor of Mechanical Engineering
Brendon C. Allen, Assistant Professor of Mechanical Engineering
Jaimie A Roper, Associate Professor of Kinesiology

Abstract

Neurological conditions such as stroke often result in motor impairments that limit functional independence and quality of life. Neurorehabilitation aims to restore motor function through intensive, repetitive therapy, relying increasingly on technologies that provide objective measures and therapeutic assistance. Among these, functional electrical stimulation (FES) is a widely used technique that activates paralyzed or weakened muscles to produce functional movements and promote recovery. However, a significant limitation of FES is the rapid onset of muscle fatigue, which shortens the duration of effective contractions, reducing the therapeutic benefits of treatment. Addressing this challenge requires reliable, real-time monitoring of fatigue to enable adaptive control of stimulation parameters.

This thesis investigates mechanomyography (MMG) as a robust, low-cost tool for detecting muscle fatigue during both static and dynamic tasks. Experimental studies showed that MMG features reflected fatigue development in static contractions and continued to perform reliably during dynamic movements. A direct comparison between MMG and electromyography (EMG) revealed that MMG offers comparable sensitivity to fatigue-induced changes while avoiding several practical limitations inherent to EMG recordings. A fatigue-thresholding method using MMG signal features was proposed for integration into real-time FES control systems, aiming to adjust stimulation parameters dynamically to prolong effective contractions. Overall, the findings highlight MMG's potential to improve fatigue detection and support next-generation neurorehabilitation technologies like adaptive FES.

Acknowledgments

I'd like to thank the many people who made my graduate school experience what it was. First and foremost, I'm incredibly grateful to my advisor, Dr. Chad Rose, for letting me join the WeBR lab despite my disastrous 2/10 on the first Systems quiz, and for talking me off the ledge more times than I can count since then. Thank you to Dr. Brendon Allen and Dr. Jaimie Roper for their time and assistance in serving on my committee. Shoutout to my fellow WeBR labmates, your camaraderie made the past two years infinitely more bearable. Thank you to the Alabama Space Grant Consortium (ASGC) for funding my research and making it possible for me to spend two unforgettable weeks at NASA's Johnson Space Center. Huge thanks to Chris Beck and everyone in the HumanWorks Lab for welcoming me so warmly and being willing participants in my experiment. Finally, to my friends and family: thank you for your constant support and encouragement through it all. Special shoutout to my sisters, Lucy and Ellie, for always believing in me, and to my dad, who's been my biggest fan from the beginning. I probably wouldn't even be an engineer if not for him.

Table of Contents

Abstract ii

Acknowledgments iii

List of Figures vii

List of Tables xi

List of Abbreviations xii

1 Introduction 1

1.1 Background 1

1.2 Review of Methods for Muscle Fatigue Analysis 5

1.2.1 Subjective Fatigue Ratings 5

1.2.2 Force 6

1.2.3 Electromyography 8

1.2.4 Ultrasound 10

1.2.5 Mechanomyography 10

1.3 Thesis Outline 12

2 Sensor Development 14

2.1 Survey of MMG Sensor Technologies 14

2.1.1 Condenser Microphones 14

2.1.2 Piezoelectric Contact Sensors 15

2.1.3 Accelerometers . . . 15
2.2 Sensor Selection . . . 16
2.2.1 Justification . . . 16
2.2.2 Sensor Specifications . . . 16
2.3 Sensor Setup . . . 17

3 MMG During Static Contractions . . . 20
3.1 Introduction . . . 20
3.2 Materials and Methods . . . 21
3.2.1 Participants . . . 21
3.2.2 Experimental Protocol . . . 22
3.2.3 Data Acquisition and Signal Processing . . . 23
3.2.4 Feature Extraction . . . 25
3.3 Results . . . 26
3.4 Discussion . . . 28
3.5 Limitations . . . 29
3.6 Future Work . . . 30
3.7 Conclusion . . . 31

4 MMG During Dynamic Contractions . . . 33
4.1 Introduction . . . 33
4.2 Materials and Methods . . . 34
4.2.1 Participants . . . 34
4.2.2 Experimental Protocol . . . 34
4.2.3 Data Acquisition and Signal Processing . . . 36
4.3 Results . . . 38
4.4 Discussion . . . 41

4.5 Limitations . . . 43
4.6 Future Work . . . 44
4.7 Conclusion . . . 45

5 Case Study: EMG Comparison . . . 46
5.1 Introduction . . . 46
5.2 Materials and Methods . . . 48
5.2.1 Participant . . . 48
5.2.2 Experimental Protocol . . . 48
5.2.3 Data Acquisition and Signal Processing . . . 48
5.3 Results . . . 50
5.4 Discussion . . . 51
5.5 Limitations . . . 54
5.6 Future Work . . . 55
5.7 Conclusion . . . 56

6 Conclusion . . . 57
6.1 Future Work . . . 58
6.2 Conclusion . . . 59

Appendices . . . 60
A.1 Python Data Acquisition Script . . . 60
A.2 MATLAB Processing Script . . . 64

References . . . 66

List of Figures

1.1 Proportional contribution of common neurological conditions to the total disability-adjusted life-year burden attributed to neurological disorders worldwide. Stroke dominates at 42.2%. Figure reproduced from [1]. 2

1.2 Schematic illustration of Henneman's size principle. During a voluntary contraction, motor units are recruited in an orderly, size-dependent sequence: small, fatigue-resistant (slow-twitch) units are activated first, and progressively larger, fast-twitch units are added only as greater force is required. Figure reproduced from [2]. 4

1.3 Representative equipment used to measure muscle force/torque: (a) Biodex isokinetic dynamometer [3], which delivers controlled-velocity joint motions while recording torque, and (b) Jamar hand-grip dynamometer [4], a compact tool for assessing static grip strength. 8

1.4 Multi-electrode surface EMG setup for upper limb muscle analysis. Low profile wireless sensors are placed over the muscle bellies to capture muscle activity while allowing unrestricted movement. Figure reproduced from [5]. 9

1.5 Representative cart-mounted diagnostic ultrasound platfrom with handheld probe. The wheeled console integrates power supply, high-channel beam-former electronics, and a display/controls unit, illustrating the infrastructure requirements that limit portability. 11

1.6 Conceptual overview of the proposed MMG-based fatigue monitoring and FES control framework. As the muscle activates, a wearable sensor captures its mechanical vibrations and which are then transmitted to a computer for signal processing. Time and frequency features are then extracted to determine the onset of muscle fatigue. Although this thesis focuses on developing the fatigue measure, the end goal is to incorporate this metric into a real-time controller for FES systems. 13

2.1 Analog Devices ADXL 367, an ultra-low-power, three-axis MEMS accelerometer. The central black QFN package houses the sensing element and on-chip signal conditioning, while the surrounding castellated pads and vertical pin header expose power SPI/I^{2}C interface, and interrupt lines. The compact 18 mm x 18 mm PCB keeps added mass below 2 g [6]. 17

2.2 Mechanomyography signal acquisition and processing workflow used throughout this thesis, Muscle activation is first converted into triaxial acceleration by a lightweight ADXL367 sensor, and the raw signal is streamed to a Raspberry Pi Pico, where it is time-stamped and saved as a CSV file. Offline MATLAB algorithms apply a 4th order Butterworth bandpass filter, then perform temporal and spectral feature extraction to compute a fatigue criterion that drives subsequent analyses. 18

3.1 Experimental setup for capturing MMG signals during a static dumbbell hold. The participant maintains the posture shown with an accelerometer placed over the muscle belly to record the mechanical vibrations. The coordinate system illustrated indicates the x, y, and z axes. Real-time visual feedback of the dumbbell's position is provided to help maintain proper posture throughout the trial. . 23

3.2 Comparison of the raw (top) and filtered (bottom) MMG signals in the Z-axis recorded from the accelerometer. The filter is designed to capture the typical frequency band at which oscillations occur, resulting in a cleaner signal. 24

3.3 Group-averaged RMS (top row) and MPF (bottom row) features computed from the acceleration magnitude of MMG signals during sustained isometric contractions at 20%, 40%, and 80% of MVC. All values are plotted over normalized endurance time. Shaded regions represent standard deviation across participants. Across all conditions, RMS increases while MPF decreases over time, reflecting consistent patterns of fatigue development. 26

3.4 Representative trial illustrating the dual-criterion fatigue detection method. RMS (top) and MPF (bottom) signals are plotted over normalized endurance time, with dashed lines indicating the 40% RMS increase and 3% MPF decrease thresholds. Fatigue onset is identified at the point where both features simultaneously exceed their respective thresholds, marked by the vertical dotted line and open circles. This approach enhances robustness by requiring sustained changes in both time- and frequency-domain features before classifying the onset of fatigue. 27

4.1 BeyondPower Voltra training system. (A) Motor-controlled resistance unit secured to a rack; the cable applies programmable load while integrated sensors record force and displacement [7]. (B) Beyond+ mobile application displaying exercise metrics such as range of motion, repetition velocity, and mechanical powe [8]. 35

4.2 The participants performed standing bicep curls with the non-dominant arm while the BeyondPower Voltra unit (mounted at the base of the rack) supplies cable resistance through a D-handle. The upper arm is braced agaisnt the rack to minimize shoulder motion, esuring that elbow flexors do the primary work. An ADXL367 accelerometer secured to the bicep records MMG, and the Voltra's onboard sensors track force and kinematics for evvery repetition. 36

4.3 Group-averaged MMG RMS and MPF trajectories across three dynamic resistance sets. Top panels show the mean normalized RMS amplitude over the course of each set, with shaded regions representing ±1 standard deviation. RMS generally increases during the early portion of each set, remains elevated through the middle, and declines near the end, consistent with increased motor unit recruitment followed by fatigue-related output loss. Bottom panels display mean MPF trajectories across time, with a gradual decline in frequency observed in all three sets, reflecting slowed neuromuscular dynamics as fatigue accumulates. These patterns were consistent across participants despite inter-individual variability. 38

4.4 Representative MMG RMS trajectories and corresponding power output for participant P08 across three dynamic exercise sets. Top panels show normalized RMS amplitude over time, with vertical dashed lines indicating the change-points identified by the fatigue detection algorithm. Bottom panels display peak power output for each repetition within the corresponding set. In all three sets, RMS generally increases before dropping sharply near the end, aligning with declining power output. This pattern reflects the onset of neuromuscular fatigue and was consistently observed across participants. 39

4.5 Distribution of fatigue onset times across sets based on MMG RMS change-point detection. Boxplots show the percentage of total set duration at which the algorithm detected the onset of fatigue for each set. Median onset times occurred between 78–83% of the trial, with interquartile ranges indicating moderate inter-individual variability. While some participants fatigued earlier or later than others, the majority showed a consistent trend of fatigue onset in the final 20–25% of each set, supporting the robustness of the MMG-based detection method. 40

5.1 Anatomical illustrations of the forearm highlighting the muscles monitored in the study: (A) the flexor digitorum superficialis (FDS), a primary finger-flexor on the anterior forearm, and (B) the extensor carpi radialis (ECR), a principal wrist extensor on the posterolateral forearm [9, 10]. Black arrows indicate the approximate midpoint of each muscle belly where EMG sensors were placed. . 47

5.2 Experimental setup and sensor placement for the forearm-fatigue protocol. (A) The participant sat upright with elbows extended and wrists neutral, statically holding 11.3 kg dumbbells in each hand until volitional failure to induce forearm fatigue. (B) Close-up of the left forearm showing the two EMG sensors: the proximal unit is centered over the extensor carpi radialis and the distal unit over the flexor digitorum superficialis. 49

5.3 Each panel overlays acceleration magnitude (MMG, blue, left ordinate) and surface-EMG (EMG, orange, right ordinate). Top row: normalized RMS; bottom row: normalized MPF. The left column represents the non-dominant forearm, the right column the dominant forearm. In both forearms EMG shows a continuous rise in RMS accompanied by a compression of MPF, indicating progressive recruitment of fast-twitch motor units. Large-amplitude MMG bursts appear only after electrical fatigue is well established (60% of trial time in the non-dominant limb, 45% in the dominant limb), demonstrating that overt tremor lags behind its electrical precursors. 50

5.4 Plot layout and color coding are identical to Figure 5.3. Only brief, isolated MMG amplitude bursts are visible and both EMG metrics remain within ±20% of baseline, confirming that ECR served chiefly as a low-fatigue wrist stabilizer during the grip-hold. Dashed grid lines mark 20% increments of total trial time 51

List of Tables

2.1 Wiring Connections Between Raspberry Pi Pico and ADXL367 18

3.1 Participant demographics with activity (Act) and fitness (Fit) levels. 21

3.2 MVIC load and endurance time at each contraction level. 22

4.1 Participant demographics including activity (Act) and fitness (Fit) levels. 34

List of Abbreviations

ADL Activities of Daily Living

CASET Curling Artifical Soft ExoskeleTon

ECR Extensor Carpi Radialis

EMI Electromagnetic Interference

FDS Flexor Digitorum Superficialis

FES Functional Electrical Stimulation

IRB Institutional Review Board

MMG Mechanomyography

MVIC Maximum Voluntary Isometric Contraction

NC Neurological Conditions

ROM Range of Motion

SCI Spinal Cord Injury

Chapter 1

Introduction

1.1 Background

Neurological conditions (NCs) such as stroke and spinal cord injury (SCI), among others, are the leading cause of long-term disability worldwide [1]. It is estimated that nearly one in three people will experience some form of neurological disorder in their lifetime, and the combined economic burden of direct medical care, lost productivity, and informal caregiving is measured to be trillions of dollars each year [11]. Figure 1.1 highlights how this burden is concentrated: stroke alone is responsible for 42.2% of all disability-adjusted life years lost to NCs. At the same time, the workforce needed to deliver intensive rehabilitation is struggling to keep up with demand. A recent analysis of the U.S. physical therapy workforce projects a persistent shortfall of licensed physical therapists through at least 2037, with supply expected to remain below need by several thousand practitioners even in the best case scenarios [12]. This mismatch between rising disability prevalence and limited clinical capacity makes the development of technologies that can extend therapeutic reach and efficacy all the more important.

The chronic motor impairments resulting from NCs diminish an individual's ability to perform Activities of Daily Living (ADL) and thus impede independence. Following the acute medical phase, rehabilitation aims to restore mobility and motor function; however, therapy outcomes strongly depend on the *dosage* (total number of repetitions) and *intensity* (mechanical or metabolic workload) of therapeutic exercise [13]. Studies in stroke recovery have shown that patients who engage in more repetitions and higher-intensity training tend to achieve better functional outcomes, reflecting fundamental principles of activity dependent neuroplasticity [14]. In traditional therapist guided sessions, it is often challenging to achieve the high repetition counts that experimental studies suggest are ideal for driving neuroplastic recovery [15].

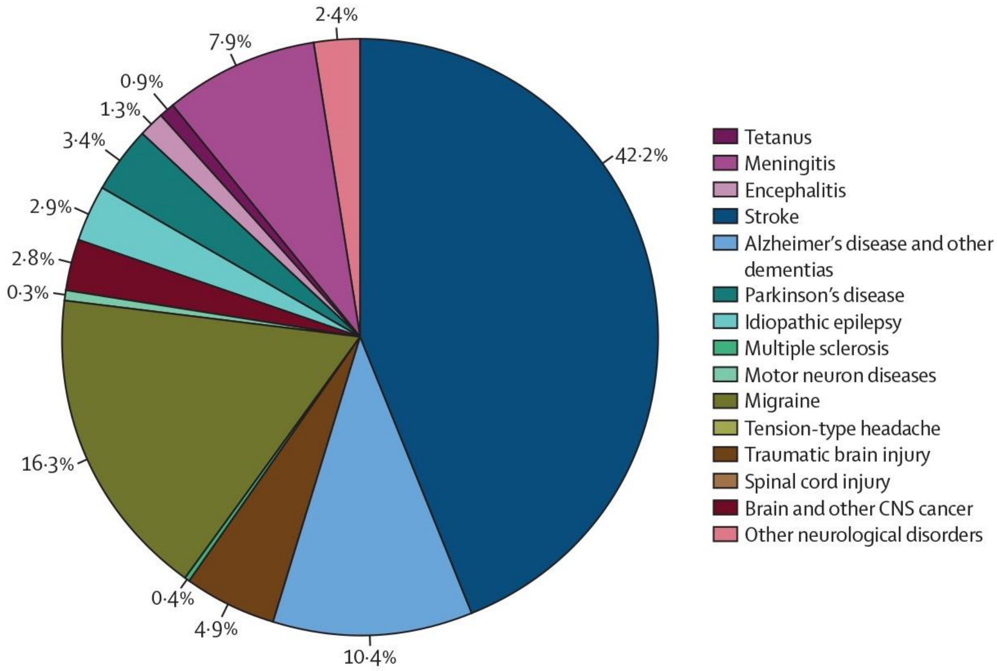

Figure 1.1: Proportional contribution of common neurological conditions to the total disability-adjusted life-year burden attributed to neurological disorders worldwide. Stroke dominates at 42.2%. Figure reproduced from [1].

This is especially true for patients with severe paralysis who cannot voluntarily activate their affected muscles to a significant degree. Furthermore, patient progress is commonly tracked using coarse clinical rating scales that lack the resolution to capture subtle improvements in motor function [16]. This lack of detailed feedback makes it difficult to personalize interventions or quantitatively assess early signs of recovery. The combination of limited therapy dose and imprecise outcome measures highlights an urgent need for new methods that can both augment patients' active practice and precisely monitor changes in neuromuscular function.

One technique to address this gap is Functional Electrical Stimulation (FES). FES is a well-established neurorehabilitation method that uses controlled pulses of electrical current to stimulate intact peripheral nerves, eliciting muscle contractions even when voluntary control is lost [17]. FES enables task-specific practice, such as grasping or cycling, by artificially activating paralyzed or weak muscles so the patient can perform a functional movement that may otherwise be impossible. This added capability allows therapists and patients to increase the number of movement repetitions and intensity of muscle use during therapy. For example, studies have shown that FES-assisted training can improve muscle strength and endurance in individuals with paralysis, enabling functional tasks after consistent practice with FES support [18, 17]. In this way, FES can augment both the quantity and quality of therapeutic exercise, which are key drivers of neuroplastic recovery. A major challenge to prolonged FES use, however, is the rapid onset of muscle fatigue during stimulation [19]. Fatigue is a multifaceted decline in the muscle's ability to generate force or power and it can arise from multiple mechanisms. These include central fatigue, originating from diminished neural drive in the brain or spinal cord; peripheral fatigue, involving impaired action potential transmission or excitation-contraction coupling at the muscle fiber; metabolic fatigue, due to depletion of ATP and accumulation of byproducts; and mechanical fatigue, related to structural failure in the contractile machinery [20]. This thesis focuses primarily on peripheral and mechanical fatigue, as detected through changes in muscle oscillations.

Under normal physiological conditions, motor units are recruited according to Henneman's size principle: smaller, fatigue-resistant motor units activate first and larger, fast-twitch units are added only as task demand rises [21]. Figure 1.2 illustrates this orderly progression. In contrast, electrically evoked contractions do not follow this orderly recruitment. External stimulation tends to recruit motor units in a non-selective or even reversed order, often activating larger, fast-fatiguing fibers at the beginning, leading to quicker fatigue accumulation in the muscle compared to volitional exercise [19].

To counteract the FES-induced fatigue barrier, researchers have explored a variety of strategies to prolong muscle performance under stimulation. One approach is to use multi-electrode setups that spatially distribute activation across different portions of a muscle. By rotating or asynchronously activating multiple electrode contacts, different muscle fiber groups can be stimulated in an alternating pattern, allowing some fibers to rest while others contract. This method has been shown to delay the decline in force output compared to using a single electrode site [22]. Beyond hardware configurations, other approaches involve adaptive or closed-loop control of FES parameters to optimize performance. In these methods, stimulation intensity, frequency, or pulse patterns are automatically adjusted to deliver just enough stimulation to achieve the desired movement while minimizing unnecessary muscle activation. Studies indicate that fine-tuning the pulse parameters and incorporating feedback can improve fatigue

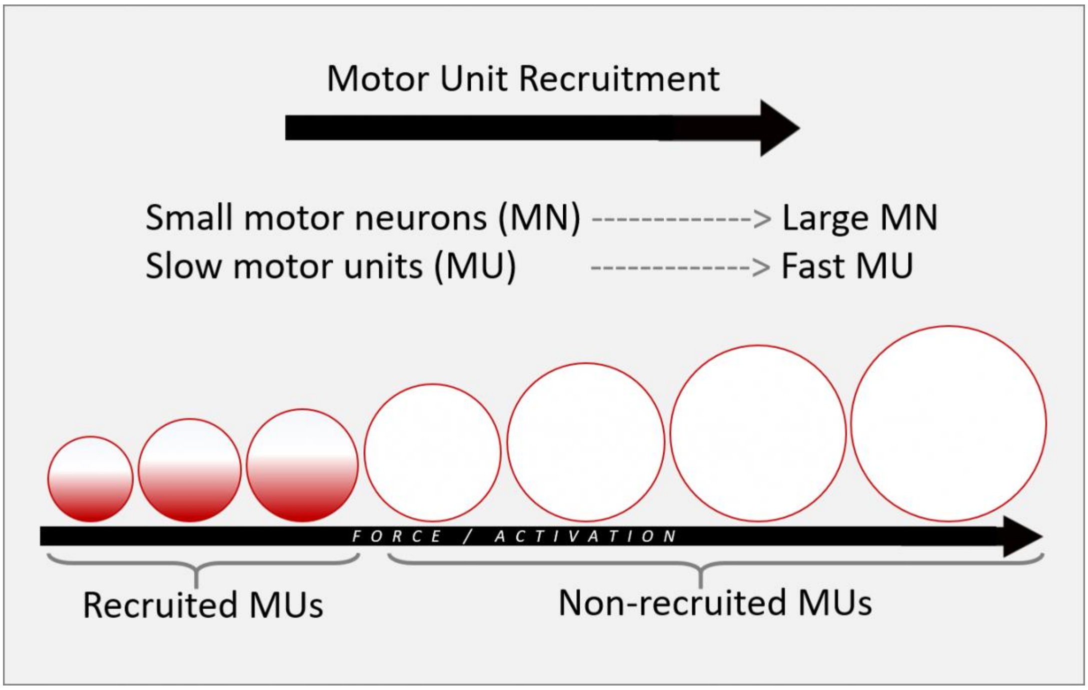

Figure 1.2: Schematic illustration of Henneman's size principle. During a voluntary contraction, motor units are recruited in an orderly, size-dependent sequence: small, fatigue-resistant (slow-twitch) units are activated first, and progressively larger, fast-twitch units are added only as greater force is required. Figure reproduced from [2].

resistance during FES exercise [23, 22]. Mitigating FES-induced fatigue is therefore critical for unlocking the full therapeutic potential of the modality. With more fatigue-resistant systems, patients could train longer and at higher intensities, potentially leading to greater functional gains over the course of rehabilitation.

Analogous neuromuscular deficits arise in astronauts exposed to microgravity. Long-duration exposure to microgravity causes physiological deconditioning of multiple systems, notable the neuromuscular and musculoskeletal systems. Without gravity's loading, astronauts experience significant muscle atrophy and loss of bone mineral density, similar to an extreme form of disuse syndrome [24]. Even with rigorous in-flight exercise protocols, extended missions inevitably lead to measurable declines in muscle strength and endurance, as well as impairments in neuromotor coordination and balance upon return to Earth [25]. NASA's rehabilitation teams accordingly implement intensive post-flight therapy: crewmembers undergo roughly 6 weeks of daily rehabilitation, including about 2 hours per day of progressive physical training to restore their pre-flight levels of motor function [26].

From an engineering perspective, the constraints of spaceflight have driven interest in compact, low-mass exercise technologies. NASA experts emphasize that any device which is smaller, lighter, and capable of multiple functions will be favored for future missions due to the premium on spacecraft resources [27]. In this context, FES-based exercise systems present an intriguing solution: because FES can activate muscles without heavy weights or large resistance machines, it could provide efficient strength training stimulus in microgravity. A lightweight FES apparatus might help maintain muscle conditioning while reducing the bulk of exercise hardware, potentially shortening the daily exercise time needed or even accelerating post-flight recovery of muscle function.

Collectively, these challenges motivate new methods for quantifying muscle activation and fatigue to guide FES protocols for terrestrial neurorehabilitation and spaceflight applications. Innovations in sensing and adaptive control of muscle stimulation hold promise for extending therapeutic efficacy of rehabilitation beyond what is currently achievable with traditional methods.

1.2 Review of Methods for Muscle Fatigue Analysis

A variety of tools have been explored to track muscle fatigue; however, each presents distinct trade-offs with respect to accuracy, cost, and ease of use. This section discusses subjective fatigue ratings, force measurement tools, electromyography, ultrasound, and mechanomyography. Currently, no single modality satisfies every requirement, so researchers and clinicians often trade precision for portability or physiological insight for simplicity. Selecting or combining the right tools depends on the setting, the population, and the specific information needed to guide training or rehabilitation.

1.2.1 Subjective Fatigue Ratings

Subjective scales are commonly used to rate perceived fatigue because they are easy to administer and capture the participant's experience. The Borg Rating of Perceived Exertion (RPE) is one widely used scale in both exercise and rehabilitation. It assigns a numerical rating to a person's sense of effort, exertion, and fatigue [28]. Borg RPE scores correlate with physiological measures like heart rate and have been extensively applied to monitor exercise intensity in healthy individuals and patients [29]. In resistance exercise, RPE has been proposed as an easy-to-use estimator of muscle fatigue, since it integrates multiple physiological cues of strain. For example, one study found a significant correlation between RPE scores and EMG-based fatigue monitoring during strength exercises, suggesting that perceived exertion rises with objective muscle fatigue [30].

Another subjective measure is the Fatigue Impact Scale (FIS), which assesses how fatigue affects physical, cognitive, and social activities [31]. Multi-dimensional scales like the FIS are especially used in clinical contexts to capture fatigue's broader impact. Notably, a recent review recommended the FIS (along with similar mutli-domain scales) for a more comprehensive assessment of fatigue, since simpler scales like the Fatigue Severity Scale (FSS) only address physical fatigue [16]. In other words, FIS can reflect cognitive and daily life implications of fatigue that a one-dimensional rating might miss. These subjective tools are easy and quick for patients to complete and thus prevalent in both research and practice for fatigue monitoring.

However, subjective ratings have obvious limitations. Perceived fatigue may not always align with objective neuromuscular fatigue levels. For instance, patients can under- or over-report fatigue due to motivation, pain, or confusion about the scale. Studies have noted that while questionnaires like the FIS or FSS are convenient, they provide only qualitative, low-resolution information that does not always correlate with actual performance decrements. Subjective fatigue scores are prone to variability and lack the reliability of instrumented measures [32]. Therefore, while subjective ratings are valuable for capturing the personal experience of fatigue, they are often complemented by objective methods in muscle fatigue analysis.

1.2.2 Force

Force measurement tools provide a direct way to quantify muscle fatigue as a decline in the muscle's ability to produce force or torque. By definition, muscle fatigue is "decrease in maximal force or power production in response to contractile activity", so measuring force output over time can reveal fatigue progression [33]. Common force measurement tools include:

Isokinetic Dynamometers: Large stationary dynamometers (e.g. Biodex system) that control joint movement velocity and widely used for muscle fatigability analysis. Isokinetic tests allow accurate assessment of force decline during repeated maximal contractions, either isometric or dynamic, under highly controlled conditions. Research has shown isokinetic dynamometry to be appropriate and safe even for clinical populations, providing reliable measures like peak torque and fatigue index. The drawback is that these devices are expensive, non-portable, and require a trained operator, but they offer precise and reproducible results [34].

Handheld Dynanometers: Portable handgrip dynamometers or similar handheld force gauges are widely used as a convenient alternative. They contain load cell sensors to measure force, typically in an isometric grip or push task. Despite their simplicity, handheld dynamometers have high reliability and can quickly quantify strength and fatigability in various settings [35]. In neurorehabilitation, for example, a sustained decline in grip force or time-to-fatigue measured by a handgrip device can indicate muscle endurance limits. These devices have been extensively used to assess upper-limb fatigue in patients with NCs [34]. Their affordability and ease of use make them suitable for routine fatigue monitoring.

Load Cells and Force Transducers: Load cells are versatile force sensors that can be integrated into exercise equipment or wearable setups to monitor force output continuously [36]. For instance, a load cell fixed to a resistance band or robotic manipulandum can record the force a muscle exerts during each repetition of an exercise. Time to failure or percent force drop offer objective metrics of fatigue [36]. Instrumented setups, including smart gym equipment or exoskeletons with force sensors, enable real-time fatigue assessment and can trigger feedback (e.g. stopping exercise when force falls below a threshold). The challenge is the cost associated with high fidelity sensors, which can often be hundreds of dollars and require proper calibration.

Figure 1.3 shows two devices commonly used for force sensing discussed above: a laboratory-grade isokinetic dynamometer and a portable hand-grip dynamometer. It should be noted that force-based measures of fatigue are often used as reference standards. A classic indicator is the decline in maximum voluntary contraction (MVC) force over a fatiguing task. Force measurements are straightforward to interpret, but they measure the outcome of fatigue rather than

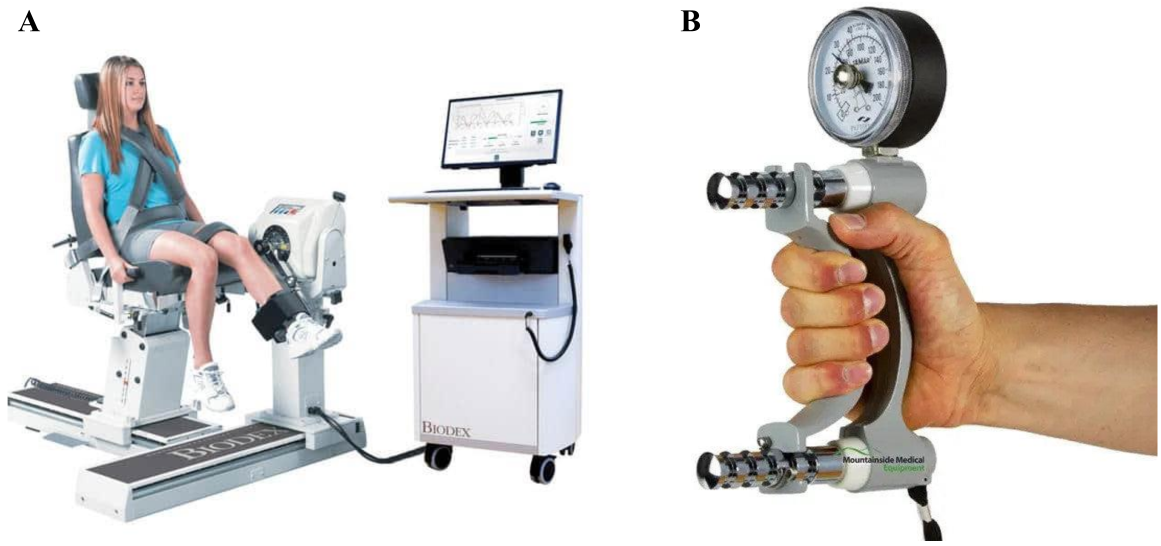

Figure 1.3: Representative equipment used to measure muscle force/torque: (a) Biodex isokinetic dynamometer [3], which delivers controlled-velocity joint motions while recording torque, and (b) Jamar hand-grip dynamometer [4], a compact tool for assessing static grip strength.

the physiological cause. To gain insight into underlying mechanisms (neuromuscular activation, muscle fiber changes, etc.), force data is frequently combined with other methods like electromyography or ultrasound imaging.

1.2.3 Electromyography

Electromyography is a core technique for analyzing muscle fatigue by recording electrical signals from muscle fibers. There are two primary types of EMG: surface EMG (sEMG) and needle EMG. Surface EMG, which uses electrodes secured to the skin, is non-invasive and widely used to monitor neuromuscular activity during fatiguing exercises [37]. Figure 1.4 shows a representative arrangement of sEMG sensors for upper extremity muscle analysis. As a muscle fatigues, characteristic changes occur in the EMG signal due to physiological factors such as muscle fiber conduction slowing and motor unit recruitment shifts. EMG fatigue metrics commonly include a decrease in frequency content of the signal and in increase in amplitude-based measures over the course of sustained activity [38]. These parameters have been widely

Figure 1.4: Multi-electrode surface EMG setup for upper limb muscle analysis. Low profile wireless sensors are placed over the muscle bellies to capture muscle activity while allowing unrestricted movement. Figure reproduced from [5].

reported in literature, providing insight into the muscle's electrical behavior as it tires [39]. In contrast, needle EMG involves inserting a fine wire or needle electrode directly into the muscle to record activity from individual motor units. While invasive and less suitable for continuous monitoring, needle EMG provides higher spatial resolution and is often used clinically for diagnosing neuromuscular disorders [40]. It offers detailed information about motor unit firing patterns, recruitment, and pathological behavior at the single-fiver level. Overall, EMG is a powerful tool for fatigue monitoring and has been applied in sports, ergonomics, and rehabilitation for decades.

However, EMG analysis is not without challenges. Signal quality can be affected by factors such as electrode placement, skin impedance, and poor preparation can mask genuine physiological changes [41]. Furthermore, using EMG in scenarios involving Functional Electrical Stimulation adds another complication. When electrical stimulators activate a muscle, the EMG electrodes pick up large stimulation artifacts that can saturate the signal and obscure underlying myoelectric activity [42]. Researchers have developed techniques to deal with this interference, such as using filtering methods to remove the known stimulus frequency components, however obtaining reliable fatigue tracking in practical FES applications remains difficult [43, 44]. While EMG is an important fatigue analysis method, alternative or supplementary signals are often considered when external stimulation is involved due to EMG's sensitivity to electrical interference.

1.2.4 Ultrasound

Diagnostic ultrasound imaging of muscle is an emerging method to evaluate muscle activity and fatigue. Ultrasound offers visualization of muscle morphology and movement beneath the skin [45]. A probe aimed at the belly of a contracting muscle can track fascicle length, pennation angle, and tissue strain, and speckle-tracking or echogenicity metrics have been shown to mirror fatigue-related declines in force during both voluntary and FES-evoked tasks [46, 47]. Because sound waves penetrate deeper than surface electrodes, ultrasound can monitor muscles that sEMG cannot reach and is immune to the electrical artifacts that plague EMG during stimulation.

The trade-off is cost and complexity. High quality cart-based scanners, shown in Figure 1.5, routinely cost tens of thousands of dollars and even newer handheld units remain far more expensive than other alternatives; historically, system price and size have limited the use of ultrasound for point-of-care fatigue monitoring [48]. Acquiring useful data also demands a skilled operator to maintain probe position, a high frame rate to capture rapid tissue motion, and intensive image processing pipelines. Most fatigue studies therefore rely on offline analysis rather than true closed-loop control [49, 50]. These hardware and computational burdens make real-time ultrasound based fatigue feedback feasible today only in tightly controlled laboratory settings.

1.2.5 Mechanomyography

Mechanomyography (MMG) is the technique of measuring the mechanical vibrations produced by muscles during contraction. When muscle fibers activate, they generate small lateral oscillations in the muscle belly [51]. MMG sensors, typically accelerometers or low-frequency

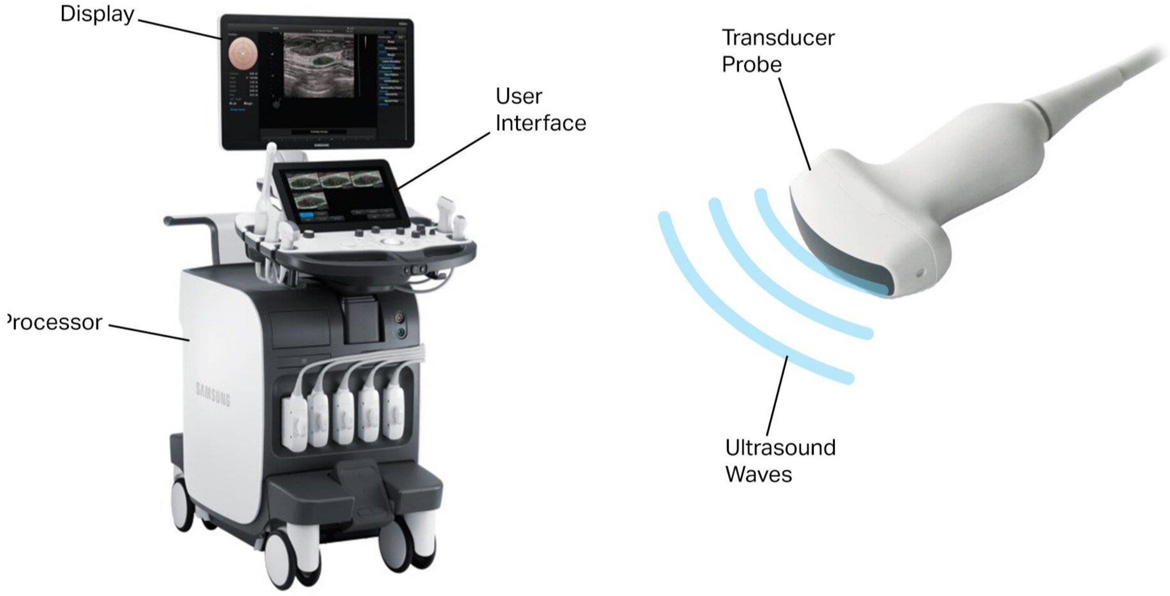

Figure 1.5: Representative cart-mounted diagnostic ultrasound platfrom with handheld probe. The wheeled console integrates power supply, high-channel beam-former electronics, and a display/controls unit, illustrating the infrastructure requirements that limit portability.

microphones attached to the skin, capture these mechanical signals. The MMG signal can be thought of as the physical counterpart to the EMG signal: instead of electrical activity, it reflects the muscle's mechanical response as motor units fire. MMG is sensitive to changes in muscle fiber contraction dynamics and exhibits characteristic signal changes as a muscle fatigues [52]. Trends in MMG have been shown to parallel those in EMG in many cases, giving MMG a physiological interpretability similar to that of EMG but from purely mechanical data [53, 54]. MMG can provide a rich source of information on muscle fatigue, capturing aspects like muscle tremor, firing rate changes, and motor unit recruitment shifts from a mechanical perspective.

One of the biggest advantages of MMG for certain applications is that it is immune to electrical artifacts. Unlike EMG, MMG is not affected by electromagnetic interference from FES pulses or other electronic equipment [55]. This makes MMG extremely attractive for wearable fatigue monitors and FES-integrated systems. In scenarios such as FES-assisted exercise where EMG is unreliable due to stimulation artifacts, MMG can reliably capture the mechanical response of the muscle without contamination. Overall, MMG is a promising method for muscle activity analysis, especially when wearability and FES-compatibility are concerns. It is non-invasive and inexpensive, and because it measures mechanical vibration, can be used when EMG or other methods are not feasible. Researchers have concluded that MMG is a valid and reliable measure of muscle activity, and they encourage further development of MMG-based wearables for rehabilitation [56].

1.3 Thesis Outline

This thesis is structured as follows: Chapter 2 details the rationale for selecting an accelerometer-based sensor, the sensor setup used throughout this work, and the procedure for signal acquisition and processing. Chapter 3 investigates mechanomyography behavior during sustained isometric contractions, establishing signal characteristics and fatigue markers. Building on these results, Chapter 4 extends analysis to dynamic contractions. Chapter 5 integrates sEMG with MMG in a fatiguing protocol, offering a comparative case study that explores the complementary information provided by electrical and mechanical muscle activity. Chapter 6 synthesizes experimental outcomes and outlines directions for translating MMG-based fatigue metrics into closed-loop, real-time control schemes. Collectively, this work validates MMG as a viable tool for fatigue assessment and provides a methodological framework for its future integration into assistive and rehabilitative devices. Figure 1.6 offers a visual representation of the thesis contributions.

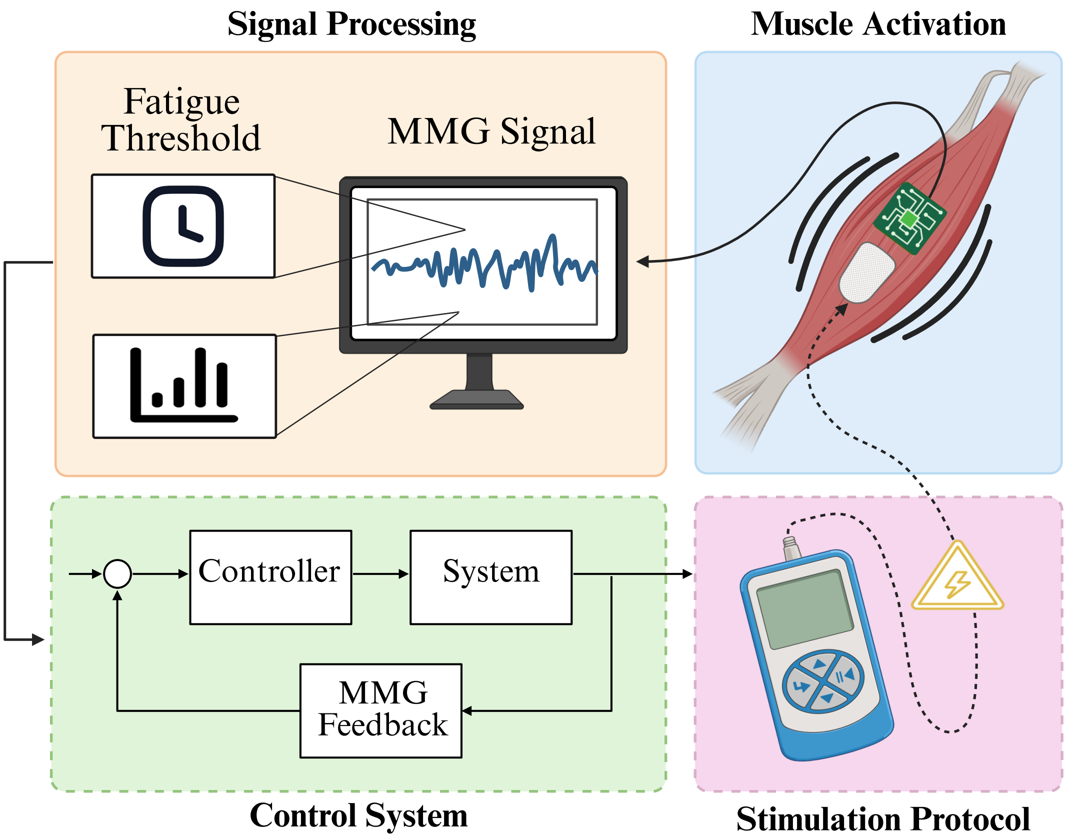

Figure 1.6: Conceptual overview of the proposed MMG-based fatigue monitoring and FES control framework. As the muscle activates, a wearable sensor captures its mechanical vibrations and which are then transmitted to a computer for signal processing. Time and frequency features are then extracted to determine the onset of muscle fatigue. Although this thesis focuses on developing the fatigue measure, the end goal is to incorporate this metric into a real-time controller for FES systems.

Chapter 2

Sensor Development

Muscle generated oscillations can be measured by local pressure waves, surface displacement, or linear acceleration, and each physical manifestation lends itself to a distinct sensing technology [57]. Selecting an appropriate device therefore requires a balanced consideration of bandwidth, power demand, and overall robustness in a clinical or home-based environment. Sensor mass is also a critical parameter. A comparative study of the signal obtained from the rectus femoris from sensors of varying masses shows that MMG sensors should weigh no more than 13 grams, as heavier sensors can dampen the muscle signal [58]. Any sensor intended for long-term, wearable use must therefore be both mechanically lightweight but also robust enough to withstand repeated use. The following chapter outlines the principal options that have appeared in MMG literature and describes the sensor used in the present work.

2.1 Survey of MMG Sensor Technologies

2.1.1 Condenser Microphones

Early MMG studies relied on condenser microphones pressed lightly against the skin. These tiny transducers are extremely sensitive to pressure waves in the 5-100 Hz range where most MMG energy resides, and their mass is negligible such that they do not significantly load the tissue [59]. However, microphones are equally sensitive to airborne noise and handling artifacts. External sounds, cable rubbing, or even a clinician's voice can be picked up by the microphone, complicating recordings unless measurements are taken in a sound-treated room [60]. Condenser microphones also require a dedicated preamplifier and careful acoustic sealing against the skin. Any slight changes in the coupling can alter the recorded signal. Thus, while microphones provide excellent sensitivity, their susceptibility to ambient noise and need for controlled conditions make them less practical outside of laboratory environments.

2.1.2 Piezoelectric Contact Sensors

Piezoelectric contact sensors convert minute skin deformations directly into voltage. Even a small piezoelectric element produces a relatively large signal in response to muscle vibrations so MMG signals can be recorded without additional amplification. However, the piezoelectric ceramic is brittle and typically bonded to a stiff backing to prevent cracking and stabilize the sensor. This added mass and casing introduce inertia that can filter out the highest frequency components of the muscle vibration [61]. In practice, the sensor's own resonance can dominate the output, meaning the recorded waveform may reflect the sensor's mechanical properties as much as the muscle's true motion. While piezoelectric contact sensors have been widely used in MMG research for their simplicity and strong signal, one must be mindful that they can attenuate or distort higher frequency muscle tremor content. The sensor's bulk and the need for firm mounting can also introduce movement artifacts if not well secured.

2.1.3 Accelerometers

Contemporary investigations have shifted toward micro-electromechanical-system (MEMS) accelerometers for MMG. These tiny chips measure the linear acceleration of the muscle surface, providing a direct representation of muscle movement that is inherently immune to acoustic noise. Modern MEMS accelerometers also feature an almost flat frequency response over the MMG range, meaning they capture both low- and high-frequency muscle oscillations without the sensor coloring the signal [62]. Another practical advantage is that accelerometers can be integrated easily into wearable setups; they are robust against sweat, have on-chip signal conditioning, and weigh only a few grams. Overall, accelerometers have become the prevalent MMG sensor in recent years, especially for wearable and clinical applications, due to their small size, reliability, and insensitivity to environmental noise [63]. They offer a good balance of bandwidth and robustness, which is why the present work utilizes an ADXL367 accelerometer (Analog Devices, Norwood, MA, USA), shown in Figure 2.1, as the MMG transducer of choice. The following sections detail the technical specifications of this sensor and the data acquisition setup in this work.

2.2 Sensor Selection

2.2.1 Justification

Given the constraints of size, cost, and robustness, a MEMS accelerometer is the most balanced solution for a wearable MMG platform. Accelerometers tolerate sweat and motion, can be integrated with adhesive patches without elaborate housings, and dominate recent MMG literature, providing a large comparative database and validated processing pipelines. Their insensitivity to high-voltage pulses used in functional electrical stimulation also overcomes the stimulation artifacts that routinely contaminate surface EMG.

2.2.2 Sensor Specifications

This sensor measures tri-axial acceleration at a sampling rate of 400 Hz, has a sensitivity of ± 2 g, and is lightweight with a mass of 4 grams. While a 1000 Hz sampling rate is often reported in literature, MMG energy is typically confined to 5-100 Hz, with only sporadic components approaching 150 Hz during very rapid contractions [52]. By the Nyquist criterion, a 400 Hz output rate should cleanly capture all physiologically relevant signal content. The ± 2 g sensitivity range also provides room for motion artifacts, such as limb shifts and cable tugs which rarely exceed ± 1 g, while keeping the resolution high [64]. Operating at a lower sampling rate also reduces storage requirements and microcontroller workload, enabling longer recordings and on-board real-time feature extraction essential to eventual closed-loop FES applications. This sensor configuration balances physiological bandwidth and system level efficiency while also testing whether clinically useful MMG metrics can be obtained without the traditional 1 kHz overhead.

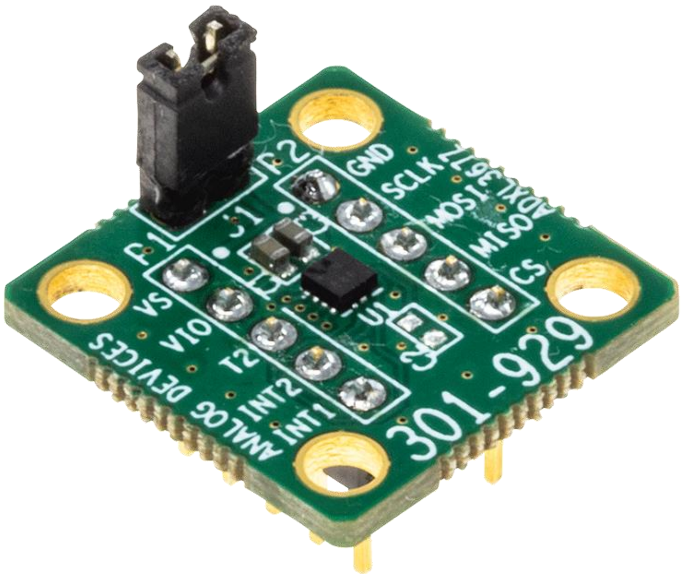

Figure 2.1: Analog Devices ADXL 367, an ultra-low-power, three-axis MEMS accelerometer. The central black QFN package houses the sensing element and on-chip signal conditioning, while the surrounding castellated pads and vertical pin header expose power SPI/I^{2}C interface, and interrupt lines. The compact 18 mm x 18 mm PCB keeps added mass below 2 g [6].

2.3 Sensor Setup

Flexible, 32-AWG silicone-enclosed wires carry power and SPI signals between the ADXL367 and a Raspberry Pi Pico microcontroller (Raspberry Pi Foundation, Cambridge, UK). Table 2.1 outlines the corresponding wiring connections between the two devices. The low mass of the sensor allows for it to be secured over the muscle of interest with double-sided adhesive without restricting natural movement. Firmware adapted from the manufacturer initializes the accelerometer, time-stamps each triaxial sample, and streams the data over USB at 400 Hz. A companion Python script running on the host computer captures the stream and writes it to a disk as a timestamped CSV file, which is presented in Appendix A.1. Once acquisition is complete, a MATLAB script is used to import the raw acceleration, apply a 4^{th} order Butterworth bandpass filter (5-100 Hz), and compute both temporal and spectral metrics as presnted in Appendix A.2. Root Mean Square (RMS) amplitude, the primary temporal feature, quantifies the magnitude of mechanical oscillations and reflects the intensity of motor recruitment. Mean Power Frequency (MPF), the primary spectral feature, indicates the average frequency content of the signal and is sensitive to changes in muscle contraction dynamics and firing rates [65].

These features are then tracked over time to identify key inflection points that signify fatigue onset. Figure 2.2 summarizes this workflow, from muscle activation through embedded acquisition to offline feature extraction and fatigue classification. The same pipeline is used in the experimental protocols described in Chapters 3 and 4, ensuring methodological consistency throughout this thesis.

Table 2.1: Wiring Connections Between Raspberry Pi Pico and ADXL367

ADXL367 Pin	Raspberry Pi Pico Pin	Function
VS	3V3(OUT)	Power Supply
VIO	3V3(OUT)	Logic Level Supply
GND	GND	Ground
INT1	GP9	Interrupt Output
SCLK	GP18	SPI Clock
MOSI	GP19	SPI MOSI (Master Out Slave In)
MISO	GP16	SPI MISO (Master In Slave Out)
CS	GP17	Chip Select

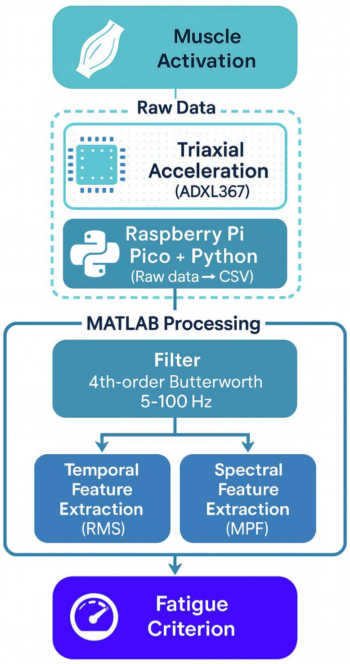

Figure 2.2: Mechanomyography signal acquisition and processing workflow used throughout this thesis, Muscle activation is first converted into triaxial acceleration by a lightweight ADXL367 sensor, and the raw signal is streamed to a Raspberry Pi Pico, where it is time-stamped and saved as a CSV file. Offline MATLAB algorithms apply a 4th order Butterworth bandpass filter, then perform temporal and spectral feature extraction to compute a fatigue criterion that drives subsequent analyses.

By pairing a state-of-the-art MEMS accelerometer with a lightweight microcontroller and an efficient data pipeline, the present system demonstrates that clinically meaningful MMG metrics can be obtained without the bandwidth, storage, and cost overhead typical of other sensor platforms, The approach lays the groundwork for future closed-loop FES applications in which real-time fatigue monitoring must coexist with electrical stimulation in uncontrolled environments [66].

Chapter 3

MMG During Static Contractions[1]

3.1 Introduction

People living with neurological conditions rarely lose strength in a uniform and consistent way. Instead, they develop abnormal muscle activation ”synergies”, recruit stronger muscles to mask weaker ones, and adopt compensatory movement patterns that gradually reinforce the very deficits they wish to overcome [67]. These complex adaptations make it difficult to pinpoint which individual muscles or joints are truly limiting a person’s functional recovery. Static, or isometric, testing offers a practical way to approach that problem. By fixing the limb in a single posture, I can analyze torque-generation capacity at a particular joint angle, expose hidden left-right asymmetries, and observe how quickly specific muscles fatigue when they cannot borrow momentum from the rest of the body.

From a training perspective, isometric work is not just a diagnostic tool. Repeated static contractions have been shown to boost peak force, stimulate muscle hypertrophy, and, in some cases, improve tendon thickness [68]. Such adaptations can translate to more efficient movement profiles during dynamic actions. Because the joint angle can be selected to match an individual’s weak range (for example, mid-range elbow flexion after stroke), isometrics let clinicians deliver targeted overload stimulus without requiring complex equipment or full-body stability.

Sophisticated fatigue estimation approaches already exist for isometric work. Several groups have used load cells to track torque decay ratios, while others have applied advanced

[1]Portions of this chapter were presented in the 2025 Modeling, Estimation, and Control Conference (MECC).

signal processing pipelines to force and FES data [69, 70]. While these methods are powerful, they rely on hardware that is relatively expensive and often confined to laboratory settings.

Mechanomyography offers a lower-cost alternative with signal processing requirements that are modest by comparison. During isometric exertion, MMG amplitude and frequency content change in characteristic ways as motor recruitment rises and fatigue sets in [71]. Tracking those changes in real-time could therefore add an objective fatigue threshold to isometric therapy sessions, help therapists decide when to pause or progress a set, and give patients an identifiable sign of improvement from week to week. This chapter therefore investigates MMG behavior during sustained isometric contractions of the elbow flexors and develops a dual-criterion fatigue threshold that integrates temporal and spectral metrics to indicate fatigue onset. We also demonstrate that a compact MMG sensor with a lower bandwidth than many devices commonly reported in literature still captures relevant signal changes during prolonged isometric contractions, underscoring MMG's practicality for both clinical and home-based rehabilitation.

3.2 Materials and Methods

3.2.1 Participants

This study was performed in accordance with the Institutional Review Board (IRB) at Auburn University (+22-559 MR 2301). Three healthy participants, free of any physical or cognitive impairments, were recruited. Key subject demographics can be found in Table 3.1. Each subject provided informed consent prior to their involvement in the experiment. Given that the current study was designed as a proof-of-concept, the sample size was kept small to demonstrate feasibility of the approach and to explore preliminary outcomes.

Table 3.1: Participant demographics with activity (Act) and fitness (Fit) levels.

ID	**Age**	**Sex**	**Ht (cm)**	**Wt (kg)**	**Act Level**	**Fit Level**
P01	24	F	163	61.2	Mod	Adv
P02	22	M	178	63.5	Light	Beg
P03	27	M	178	83.9	Mod	Adv

3.2.2 Experimental Protocol

Prior to the main experimental trials, each participant's Maximum Voluntary Isometric Contraction (MVIC) was determined using an adjustable dumbbell. Subjects were provided with a five-minute warm-up period to stretch, familiarize themselves with the equipment, and optimize their grasp. During MVIC determination, the dumbbell's weight was increased incrementally. For each increment, the participant was instructed to hold the weight in a supinated position for three seconds while maintaining a consistent posture. The heaviest weight that could be held steadily for the full duration was recorded as the participant's MVIC. After MVIC determination, a 30-minute rest period was provided to minimize the effects of fatigue before the sustained isometric tasks. The MVIC values, calculated submaximal loads, and corresponding endurance times are presented in Table 3.2.

Table 3.2: MVIC load and endurance time at each contraction level.

Participant	**MVIC**	**20% MVC**		**40% MVC**		**80% MVC**	
	(kg)	(kg)	(s)	(kg)	(s)	(kg)	(s)
P01	13.9	2.7	445	5.4	176	10.9	32
P02	15.9	3.2	333	6.4	100	12.7	18
P03	18.1	3.6	406	7.3	80	14.5	9

Following this rest period, participants performed isometric holds of the dumbbell loaded with weight corresponding to 20%, 40%, and 80% of their MVIC. These levels were chosen because they span a wide physiological range; from low-intensity effort typical of everyday tasks, through a moderate training load that stresses both endurance and strength, to near maximal effort where fatigue develops rapidly [72]. For each trial, the participant sat upright in a chair with the upper portion of the arm braced against the chair back, grasped the dumbbell in a supinated position, and maintained an elbow flexion of 90° for as long as possible. This posture was held until failure, which was defined as the instant when the participant could no longer sustain 90° of elbow flexion. Throughout each trial, a monitor displayed visual feedback of the dumbbell position to help the participant maintain the correct posture. The trial concluded once failure was reached for the given contraction level. Each participant was given a 30-minute rest period to recover between trials. Figure 3.1 illustrates the experimental setup, highlighting the participant's posture, the accelerometer placement and the real-time feedback provided during the static dumbbell hold.

3.2.3 Data Acquisition and Signal Processing

The ADXL367 accelerometer was attached to the muscle belly of the biceps brachii using medical-grade double-sided adhesive. The biceps brachii was selected for two practical reasons. First, its superficial location means that the vibration field recorded at the skin surface is dominated by the biceps itself, reducing crosstalk from the deeper brachialis or nearby shoulder musculature. Second, the muscle contains an almost even mix of type I (slow-twitch) and type II (fast-twitch) fibers, so its mechanomyographic response should capture fatigue-related behavior characteristic of both fiber types and offers a balanced representation of neuromuscular

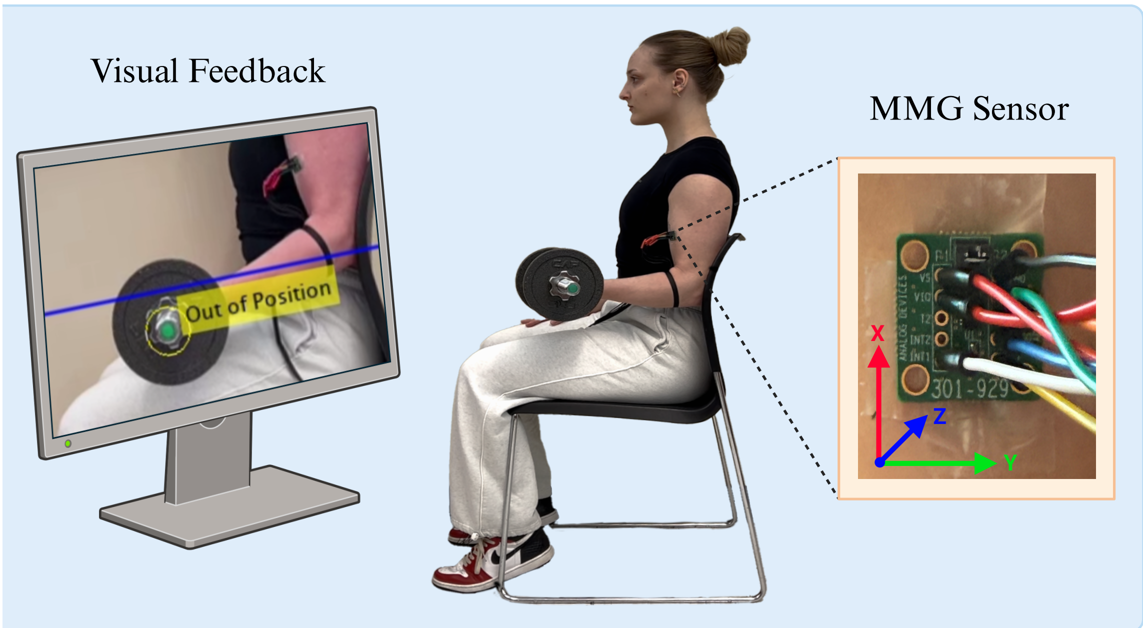

Figure 3.1: Experimental setup for capturing MMG signals during a static dumbbell hold. The participant maintains the posture shown with an accelerometer placed over the muscle belly to record the mechanical vibrations. The coordinate system illustrated indicates the x, y, and z axes. Real-time visual feedback of the dumbbell's position is provided to help maintain proper posture throughout the trial.

adaptations seen in many upper-limb tasks [73]. The placement followed standard EMG sensor location guidelines to maximize consistency between participants [74].

The accelerometer captured acceleration data along three axes at a sampling rate of 400 Hz. Data were transmitted from the sensor to a laptop via a Raspberry Pi Pico (Raspberry Pi Foundation, Cambridge, UK) and stored in .csv format with synchronized timestamps marking the beginning and end of each trial. All data processing was performed using MATLAB (MathWorks, Natick, MA, USA). To isolate the MMG content, the raw accelerometer data were band-pass filtered between 5 and 100 Hz using a 4^{th}-order Butterworth filter, a range shown to capture the dominant power of muscle vibrations while rejecting artifacts, in accordance with recommendations from previous literature [75]. Frequencies below 5 Hz are largely due to global arm sway, subtle posture adjustments, or sensor cable movement, whereas components above 100 Hz are dominated by electromagnetic interference (EMI) rather than muscle fiber oscillations. The chosen filter therefore preserves physiologically relevant MMG information while attenuating motion artifacts and high-frequency interference that could contaminate amplitude and spectral fatigue metrics. Figure 3.2 presents a comparison between the raw and filtered MMG signals recorded from the Z-axis.

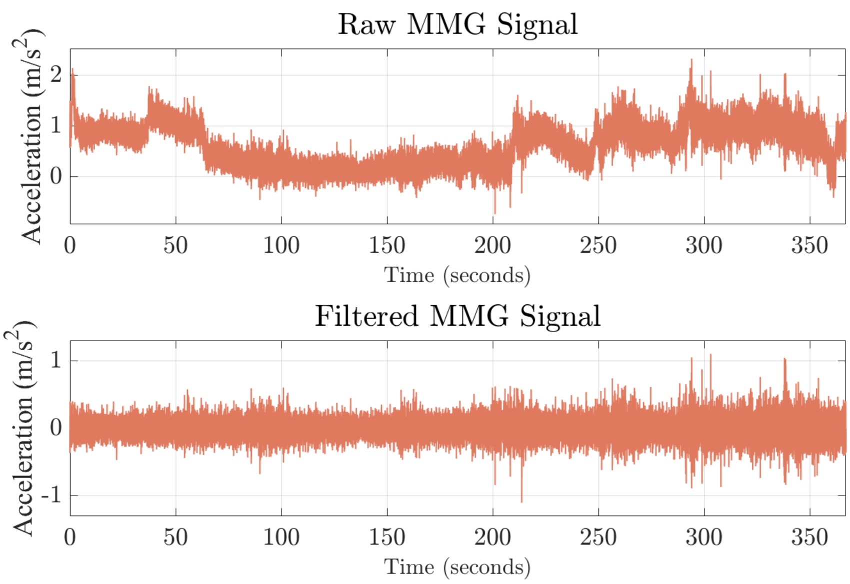

Figure 3.2: Comparison of the raw (top) and filtered (bottom) MMG signals in the Z-axis recorded from the accelerometer. The filter is designed to capture the typical frequency band at which oscillations occur, resulting in a cleaner signal.

3.2.4 Feature Extraction

Within each trial, time- and frequency-domain features were calculated using a 50-ms moving window to characterize the changing state of muscle activity over time. Specifically, the root mean square (RMS) amplitude of the acceleration signal was computed to represent changes in the overall vibration magnitude, which serves as a measure of motor unit recruitment and muscle activation. In addition, the mean power frequency (MPF) was extracted to capture shifts in the frequency content of the signal, which are indicative of changes in motor unit firing rates. Previous studies have demonstrated that while amplitude increases can signal increased effort and motor unit recruitment during the progression of fatigue, declines in MPF are associated with the slowing of muscle fiber conduction and reduced firing rates as fatigue develops [76, 53]. To further enhance the reliability of these measures, the data were smoothed using a moving average, corresponding to 10% of total endurance time, which helped to reduce transient fluctuations and noise, allowing for clearer identification of characteristic trends in the signal.

The RMS and MPF traces in this study were normalized to the mean of the first 10% of each trial, based on the assumption that the muscle was in a non-fatigued, fresh state during this period. This approach aligns with prior MMG research where baseline normalization is used to account for inter-subject and inter-session variability [77]. Furthermore, trial time was expressed as a percentage of the participant's total endurance time under a specific load. This normalization process facilitates direct comparison of muscle activity patterns across trials with varying absolute durations, enabling a more standardized assessment of fatigue dynamics.

Our analyses revealed that features derived from the magnitude of the acceleration signal offered a cleaner profile of overall muscle activity, minimizing the effects of axis-specific noise. Figure 3.3 presents the averaged RMS and MPF of the acceleration magnitude across all participants for each of the three contraction levels (20%, 40%, and 80% MVIC). Across all trials, RMS values showed a consistent upward trend, while MPF values declined steadily, reflecting progressive fatigue. These group-level trends reinforce the suitability of RMS and MPF as core features for fatigue analysis and threshold definition.

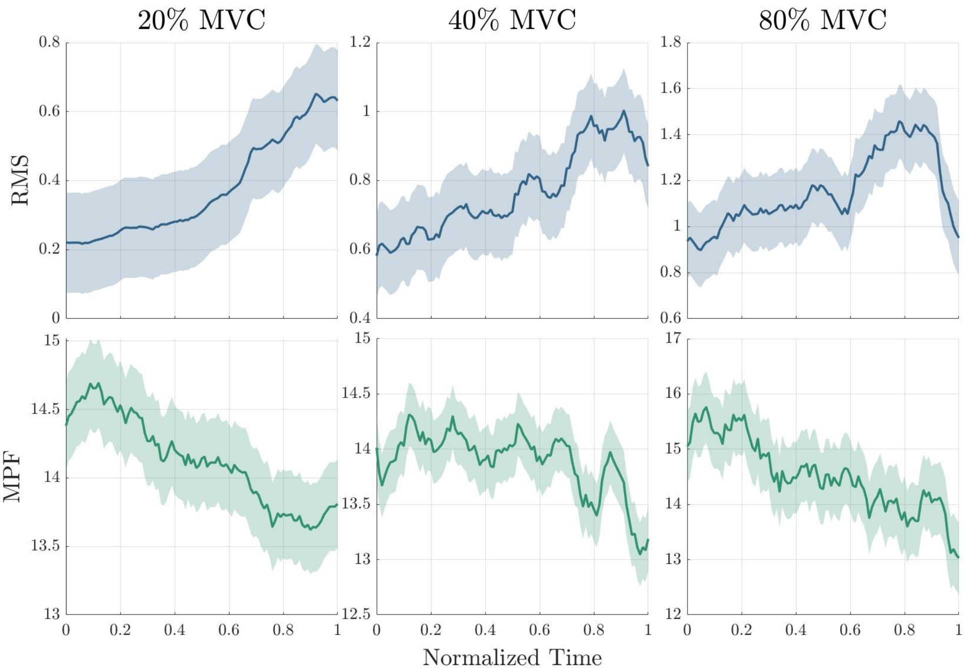

Figure 3.3: Group-averaged RMS (top row) and MPF (bottom row) features computed from the acceleration magnitude of MMG signals during sustained isometric contractions at 20%, 40%, and 80% of MVC. All values are plotted over normalized endurance time. Shaded regions represent standard deviation across participants. Across all conditions, RMS increases while MPF decreases over time, reflecting consistent patterns of fatigue development.

By focusing on RMS and MPF features, both of which are well-supported by the literature as indicators of muscle activation and fatigue, this feature extraction approach provides a framework for subsequent fatigue analysis and derivation of a fatigue threshold.

3.3 Results

Trend-based inspection of the feature trajectories in Figure 3.3 showed that fatigue consistently emerged once the RMS amplitude had increased roughly 40% above its baseline and the corresponding MPF had decreased by about 3%. To formalize this observation, the percentage change of each feature relative to the baseline values were computed in one-second epochs. The normalized curves from all trials were then superimposed, and the inflection point at which both features crossed the +40%/-3% lines was visually verified to align with the onset of visible tremor and decline in posture control that precedes failure.

These empirical boundaries were then used to develop an algorithm to identify the epoch during which three consecutive windows met both criteria, signifying the onset of fatigue. Across participants and contraction levels, this consistently occurred between 60% and 80% of the individual's endurance time, confirming the robustness of the threshold. This dual-condition requirement helped mitigate the effects of transient signal fluctuations that might otherwise be misinterpreted as fatigue. For example, isolated increases in RMS may occur due to movement artifacts or instability, while decreases in MPF could result from temporary changes in signal quality. Requiring both features to exceed their respective thresholds ensured that only sustained, physiologically relevant changes were labeled as fatigue onset. Figure 3.4 illustrates a representative trial, highlighting the progression of RMS and MPF features over normalized time and marking the point at which both thresholds are crossed. This visualization demonstrates how the dual-feature approach clearly identifies fatigue onset.

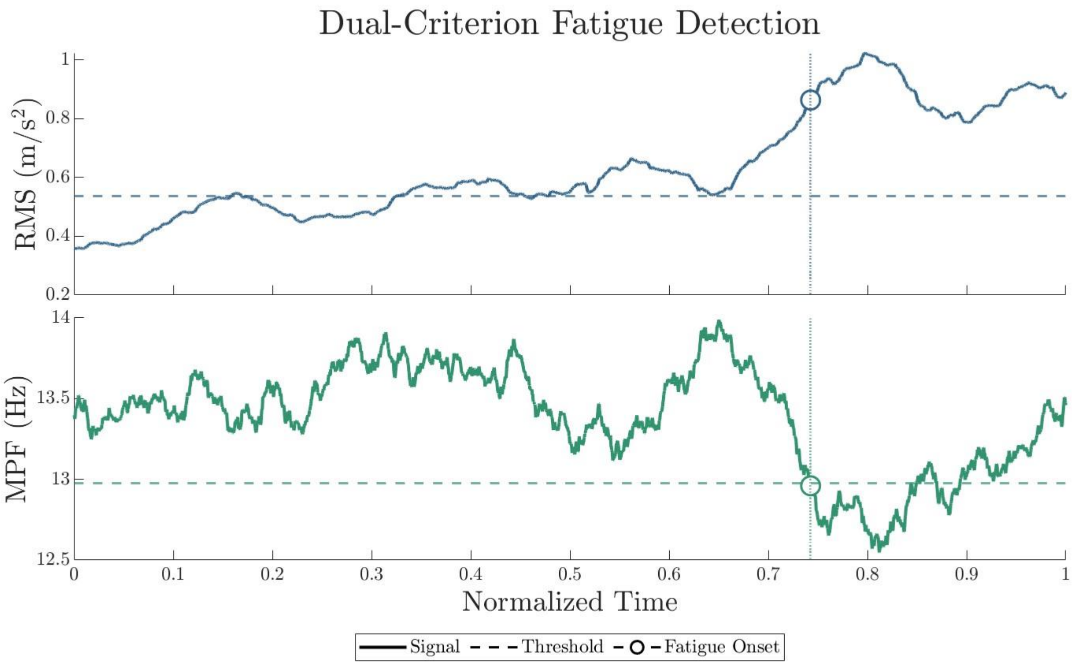

Figure 3.4: Representative trial illustrating the dual-criterion fatigue detection method. RMS (top) and MPF (bottom) signals are plotted over normalized endurance time, with dashed lines indicating the 40% RMS increase and 3% MPF decrease thresholds. Fatigue onset is identified at the point where both features simultaneously exceed their respective thresholds, marked by the vertical dotted line and open circles. This approach enhances robustness by requiring sustained changes in both time- and frequency-domain features before classifying the onset of fatigue.

Overall, this empirically defined fatigue threshold offers a simple yet effective means of identifying muscle fatigue onset using MMG signals. Its consistency across trials and sensitivity to different contraction levels suggest that it could serve as a foundation for a more comprehensive fatigue index or classifier, paving the way for real-time adaptive control strategies in rehabilitation applications.

3.4 Discussion

These results support the viability of MMG as a practical and informative tool for monitoring muscle fatigue during sustained isometric contractions. Consistent with prior work, we observed that MMG-derived features—specifically the root mean square (RMS) amplitude and mean power frequency (MPF)—undergo characteristic changes as fatigue progresses. RMS amplitude, which reflects the magnitude of mechanical oscillations associated with motor unit recruitment, consistently increased over the course of each trial. This trend is well-documented in the literature and is thought to reflect the recruitment of additional motor units to maintain force output as previously activated fibers begin to fatigue.

Simultaneously, the MPF of the MMG signal showed a consistent decline, indicative of slowing muscle contraction dynamics and reduced motor unit firing rates. This frequency-domain shift parallels similar findings in EMG literature, where reductions in median or mean frequency are attributed to decreases in conduction velocity and changes in action potential synchronization [78]. In MMG, however, the frequency shift likely reflects changes in the mechanical properties of the muscle itself, such as stiffness and damping, as well as alterations in neuromuscular control strategies [79]. The consistency of these spectral changes across trials and participants suggests that MMG-derived MPF may be a reliable metric for physiological fatigue markers.

By defining a dual-feature threshold—40% increase in RMS and 3% decrease in MPF—we were able to identify a consistent window of fatigue onset between 60% and 80% of endurance time across all conditions. This is particularly promising for real-time applications, where a fatigue indicator based on robust and interpretable features is more valuable than complex estimations that require high computational demand. Previous studies have derived fatigue thresholds from MMG signals in conjunction with external force measurements using load cells or dynamometers[a mechanomyographic]. While effective, such methods require additional hardware and calibration, which can increase system complexity and cost. In contrast, the approach presented in this paper defines the fatigue threshold directly from MMG signal features without relying on force measurements, offering a simpler and more accessible solution, especially valuable for wearable systems and settings where force-sensing equipment may not be feasible.

Overall, these results highlight MMG's potential as a low-cost, artifact-resistant, and interpretable alternative to EMG for muscle fatigue monitoring. The proposed dual-feature threshold provides a simple and effective way to detect fatigue onset in real time. With continued development, MMG-based fatigue estimation could be integrated into adaptive FES protocols to optimize stimulation parameters, prevent overexertion, and improve the efficacy and duration of rehabilitation interventions. This work lays the groundwork for such systems by demonstrating both the feasibility and reliability of fatigue detection using MMG signals under controlled conditions.

3.5 Limitations

There were several limitations in the current study that warrant discussion. First and foremost, the small sample size of three participants across a limited number of trials may have constrained the generalizability of the findings. With such a small dataset, individual variability had a larger impact on overall trends, and outlier behavior could disproportionately influence the identified fatigue thresholds. Although the consistency of the observed trends across trials was encouraging, a larger and more diverse sample would be necessary to further validate the robustness of the proposed threshold across broader populations.

Additionally, differences in participants' baseline fitness levels and muscle conditioning may have introduced variability in MMG signal characteristics. Factors such as muscle fiber composition, training history, and neuromuscular efficiency can all influence signal amplitude and spectral features, potentially affecting the timing and expression of fatigue-related changes.

While the use of normalized metrics helped to mitigate some of this variability, future studies should consider including physiological measurements such as muscle cross-sectional area or body composition to better contextualize signal patterns.

Postural control was another constraint. To keep the protocol simple and inexpensive, we did not rigidly fix the shoulder or torso. As fatigue set in, participants could have unconsciously shifted their shoulder, leaned, or swayed in such a way that altered the load distribution and, by extension, MMG characteristics. Motion-capture markers or lightweight bracing could verify posture and isolate true muscular fatigue from compensatory mechanics.

Another limitation was the use of a single sensor placed over one muscle. While the biceps brachii is a relatively isolated and commonly studied muscle, muscle fatigue often involves complex coordination across multiple synergistic and antagonistic muscles. Using multiple sensors or examining muscle groups involved in more functional, dynamic tasks could improve the validity of the approach.

3.6 Future Work

While the current thresholding method showed strong consistency, it is important to acknowledge that fatigue is a complex process that may not be fully captured by RMS and MPF alone. Future work could enhance the sensitivity and specificity of fatigue detection by incorporating additional features. Entropy-based metrics, for instance, can quantify the signal's complexity, which tends to decrease with fatigue due to more synchronized motor unit activation [80]. Time-domain metrics such as zero-crossing rate (ZCR) could further describe changes in oscillatory behavior, while joint time-frequency methods like wavelet transforms may reveal transitions that are not apparent in static time or frequency domains [81, 82].

Beyond feature engineering, advanced data-driven approaches offer another promising avenue. Machine learning classifiers, such as support vector machines (SVM) or neural networks, could be trained to recognize patterns associated with fatigue more robustly than static thresholds. These models could incorporate not only MMG features but also user-specific information and contextual cues, potentially enabling personalized fatigue monitoring systems. Moreover, regression-based models could be used to predict time to failure or remaining endurance, offering more proactive control strategies rather than simple fatigue detection.

Future work will focus on refining this threshold-based approach and developing a more comprehensive fatigue index capable of predicting the onset of fatigue before performance degradation occurs. To support this, the dataset should be expanded across a larger and more diverse participant pool, including individuals with neurological impairments, to assess clinical viability. Feature extraction will also be enhanced by exploring additional signal characteristics to capture more nuanced aspects of fatigue development. Beyond static tasks, this methodology will be extended to other muscle groups and adapted for dynamic movements to better reflect functional motor behaviors. This includes the simultaneous analysis of synergistic muscle pairs, enabling broader application in multi-joint rehabilitation settings. To further improve accuracy and enable real-time implementation, we also aim to explore advanced modeling techniques such as nonlinear regression and machine learning-based classifiers.

Translational work will focus on functional electrical stimulation (FES) applications. Mounting the forearm on a simple support and running recruitment curves at several elbow angles should allow for clean MMG data collection during FES-evoked contractions to analyze how stimulation intensity, joint angle, and fatigue interact. Coupling MMG with a load cell would add a direct mechanical reference, allowing further confirmation that the proposed MMG threshold coincides with the classically accepted decline in torque. A force transducer was not included in this study to keep costs low and demonstrate that MMG alone can identify fatigue onset, but future studies should incorporate one for validation.

3.7 Conclusion

This study presented a proof-of-concept framework for monitoring muscle fatigue in the biceps brachii using MMG signals collected via a wearable accelerometer. Our preliminary results demonstrate that time- and frequency-domain features, specifically RMS amplitude and MPF, consistently reflect fatigue progression during sustained isometric contractions. The proposed dual-feature threshold offers a simple yet effective method for detecting fatigue onset, with clear trends observed across different contraction levels and participants.

While MMG may not offer the same level of physiological detail or sensitivity as more complex methods such as EMG or ultrasound imaging, its advantages in cost, weight, and ease of integration make it an appealing option for rehabilitation applications. In many real-world or resource-limited clinical settings, it may not be feasible to deploy bulky or high-maintenance technologies. The simplicity and robustness of MMG make it especially well-suited for wearable systems and at-home therapy, where low-power and low-latency signal acquisition is essential.

Ultimately, by enabling real-time detection and response to muscle fatigue, this MMG-based approach has the potential to significantly enhance the effectiveness, safety, and personalization of rehabilitation protocols—supporting longer and more productive therapy sessions and improving outcomes for individuals with motor impairments.

Chapter 4

MMG During Dynamic Contractions

4.1 Introduction

Regaining the ability to perform purposeful, multi-joint actions is the ultimate goal of most upper-limb rehabilitation programs. Although the previous chapter focused on sustained isometric holds, ADLs usually require muscles to work through changing lengths and velocities, often under intermittent loads. Dynamic contractions involve a more complex interplay of neural drive, contractile mechanics, and limb inertia; consequently, the mechanomyographic signals generated can differ from the cleaner patterns seen during static effort [54]. Understanding these differences is essential for MMG to serve as a practical bio-signal for monitoring fatigue or controlling assistive devices in everyday activities.

Studies suggest that MMG amplitude still tends to rise and its dominant frequency still drifts downward as fatigue progresses, but the trajectories are noisier and often superimposed on large artifacts from limb movement [79]. Parameters such as contraction velocity, range of motion, and whether the action is concentric or eccentric further shape both the magnitude and spectral profile of the signal. It is therefore unclear whether the threshold values derived from static holds translate directly to tasks in which the muscle length is continuously changing. At the same time, dynamic tasks provide provide additional information that could enrich fatigue assessment if characterized properly.

This chapter explored how MMG behaves during repetitive elbow flexion and extension cycles performed at varying load levels. By comparing these recordings with the static data, the chapter aims to determine whether a similar MMG-based fatigue index can be used for dynamic activities.

4.2 Materials and Methods

4.2.1 Participants

For this proof-of-concept study, nine healthy adults with no known physical or cognitive impairments were recruited. Key demographic, anthropometric, and self-reported activity data are summarized in Table 4.1. Before participation, every volunteer provided informed consent and received step-by-step verbal and visual instructions outlining the full study procedure.

Table 4.1: Participant demographics including activity (Act) and fitness (Fit) levels.

Subject	**Age** (yrs)	**Gender**	**Ht** (cm)	**Wt** (kg)	**Act Level** Level	**Fit Level** Level
P01	24	F	163	61.2	Mod	Adv
P02	19	M	191	97.5	Very	Pro
P03	29	M	163	100.6	Mod	Pro
P04	23	M	183	70.3	Mod	Int
P05	21	M	173	68.0	Light	Beg
P06	27	F	175	95.2	Mod	Int
P07	22	F	160	56.7	Light	Beg
P08	21	M	170	72.6	Very	Adv
P09	22	M	178	81.7	Very	Adv

4.2.2 Experimental Protocol

Testing was performed with the BeyondPower Voltra resistance training unit, a compact motor-driven device that mounts to a standard power rack and applies programmable cable loads while logging kinematic data [7]. Figure 4.1 shows the device and corresponding IOS application. The system delivers motor-controlled variable resistance through a cable and automatically records metrics including range of motion (ROM), velocity, and power. Participants used a D-handle attachment and performed every task with their non-dominant arm to elicit greater muscle activation.

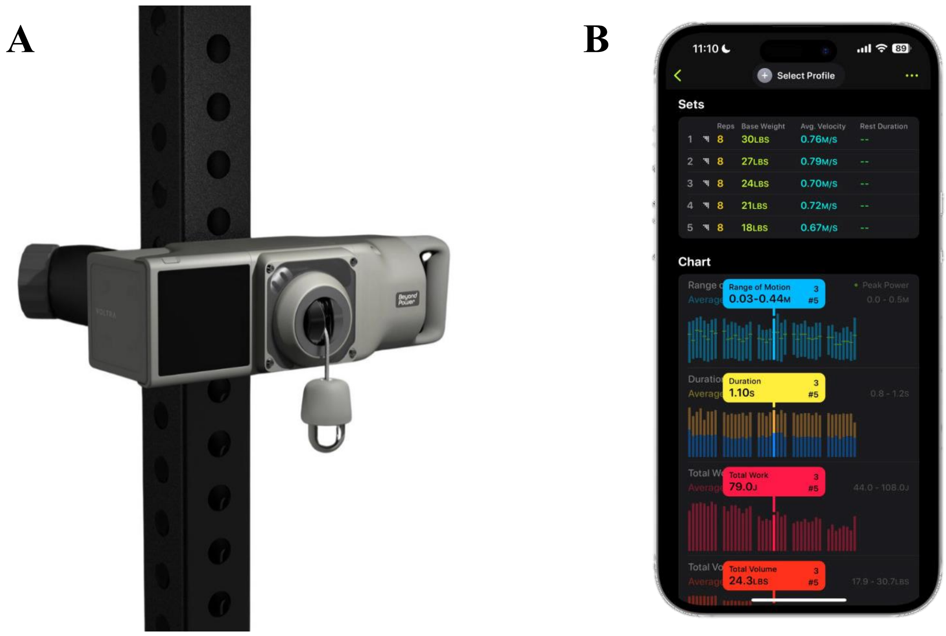

Figure 4.1: BeyondPower Voltra training system. (A) Motor-controlled resistance unit secured to a rack; the cable applies programmable load while integrated sensors record force and displacement [7]. (B) Beyond+ mobile application displaying exercise metrics such as range of motion, repetition velocity, and mechanical powe [8].

After adjusting the cable height to permit each participant a comfortable, full ROM, we provided a brief familiarization period. Each subject then executed three maximum voluntary isometric contractions (MVICs) by pulling against the locked cable with a supinated grip and maintaining the effort for two seconds. The highest force recorded across the three trials was designated as the subject's MVIC. Following a 30-minute rest period to mitigate fatigue, participants completed three sets of standing bicep curls on the same device, each targeting a distinct repetition range. Loads were adjusted such that the participant would reach failure within one to five repetitions for the first set, within six to twelve for the second, and beyond twelve for the third. These ranges emphasize, respectively, maximal strength, hypertrophy, and muscular endurance [83]. Before beginning, subjects experimented with several resistance levels to identify a load appropriate for each repetition range. During every set, subjects stood upright with the upper arm braced against the machine's rack to minimize movement from that segment, and they continued curling until they could no longer achieve a full ROM. A 30-minute recovery

Figure 4.2: The participants performed standing bicep curls with the non-dominant arm while the BeyondPower Voltra unit (mounted at the base of the rack) supplies cable resistance through a D-handle. The upper arm is braced agaisnt the rack to minimize shoulder motion, esuring that elbow flexors do the primary work. An ADXL367 accelerometer secured to the bicep records MMG, and the Voltra's onboard sensors track force and kinematics for evvery repetition.

period separated the three sets. Figure 4.2 illustrates the experimental setup, including arm bracing, sensor placement, and cable positioning.

4.2.3 Data Acquisition and Signal Processing

The ADXL367 accelerometer was attached to the muscle belly of the biceps brachii using skin-safe double-sided adhesive to ensure firm contact without restricting movement. Throughout the experiment, muscle activity was recorded while participants performed contractions on the BeyondPower Voltra resistance training device. Data from the Voltra were captured via Beyond+, an iOS application that communicates with the device over Bluetooth. Beyond+ enables the creation of individual user profiles, allowing each participant's data to be stored and exported as CSV files for further analysis.

Following data collection, CSV files from both the accelerometer and the Beyond+ application were combined for each participant and imported into MATLAB. Processing of the mechanomyography signal followed procedures consistent with earlier chapters. Raw acceleration data were converted from units of g to m/s^2 to align with standard SI units. The overall acceleration magnitude was calculated as the Euclidean norm across the x-, y-, and z-axes to yield a single, direction-independent signal.

To isolate the frequency range of interest for MMG analysis, the acceleration signals were bandpass filtered using a fourth-order Butterworth filter with cutoff frequencies selected based on prior literature to capture the dominant MMG frequency content. Signal features were then computed in 50 ms rolling windows. Within each window, root mean square (RMS) amplitude and mean power frequency (MPF) were calculated to characterize both signal intensity and spectral shifts associated with muscle activation and fatigue. All RMS and MPF values were normalized to reference levels measured during each participant's MVIC trials. Additionally, the trajectories were time-normalized relative to total trial duration, enabling comparisons across sets and participants regardless of individual trial length.

Change-point detection analysis was applied to the RMS signal to identify significant shifts that might indicate the onset of muscle fatigue or other transitions in contraction behavior. This analysis was conducted across all repetitions and sets for each participant, enabling the identification of potential fatigue thresholds or notable changes in muscle mechanical activity during exercise. Exploratory analyses were also performed on the MPF signal. Similar change-point detection methods were applied to the MPF time series to identify abrupt shifts in spectral content that might signal fatigue or altered muscle activity patterns. However, these results were less consistent than those observed in the RMS domain. As an alternative, curve-fitting techniques were employed to model MPF trajectories across repetitions, providing a characterization of spectral trends over time.

In parallel, peak power output was extracted from the Beyond+ datasets for each repetition across the three sets performed by all participants. Peak power was selected as the primary mechanical outcome rather than force measurements, as it reflects both the magnitude and speed of muscle contractions and is more functionally relevant to dynamic resistance training tasks [varying]. Peak power values were stored and linked to the corresponding MMG signal segments to facilitate combined analysis of mechanical performance metrics and muscle vibration characteristics. Batch processing routines were implemented to automate signal processing and feature extraction steps across all participants and experimental conditions, ensuring consistent and efficient data handling.

4.3 Results

Figure 4.3 shows the group-average time-course of the MMG signal amplitude (RMS) and frequency (MPF) over three exercise sets, expressed as a percentage of each set's duration. The mean curves (with shaded variability) reveal consistent fatigue-related trends across sets. In all three sets, MMG RMS initially rises or remains steady, then exhibits a marked decline toward the end of the set, whereas MMG MPF declines more gradually over time. By the final 10–20% of each set, RMS drops sharply to lower values, coinciding with the point of performance failure, while MPF reaches its lowest values. Notably, the starting MPF in later

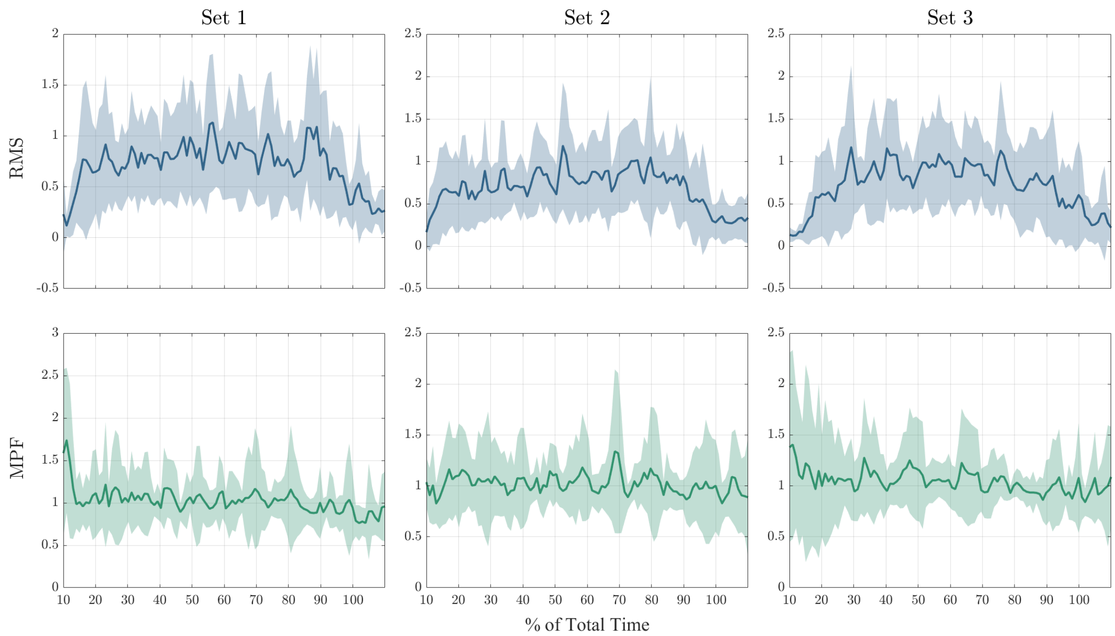

Figure 4.3: Group-averaged MMG RMS and MPF trajectories across three dynamic resistance sets. Top panels show the mean normalized RMS amplitude over the course of each set, with shaded regions representing ±1 standard deviation. RMS generally increases during the early portion of each set, remains elevated through the middle, and declines near the end, consistent with increased motor unit recruitment followed by fatigue-related output loss. Bottom panels display mean MPF trajectories across time, with a gradual decline in frequency observed in all three sets, reflecting slowed neuromuscular dynamics as fatigue accumulates. These patterns were consistent across participants despite inter-individual variability.

sets is slightly lower than in set 1, reflecting some carry-over fatigue, but the overall pattern of declining MPF and late-set RMS collapse is consistent across trials. The shaded regions indicate some inter-individual variability; however, despite some participants having higher or lower absolute RMS/MPF, the general trajectory (MPF trending downward and a late-set RMS fall) was observed in nearly all individuals, underscoring a robust group-level fatigue response.

Figure 4.4 displays the MMG RMS signal trajectory and corresponding power output per repetition across three dynamic resistance sets for participant P08. In each set, the RMS signal initially rises and stabilizes, reflecting sustained motor unit recruitment, before exhibiting a sharp decline in the final portion of the set. This inflection point, marked by a vertical dashed line, represents the statistically detected change-point and is interpreted as the onset of muscular fatigue. The lower panels show a parallel decrease in power output, with each bar representing the highest instantaneous power generated during a given repetition.

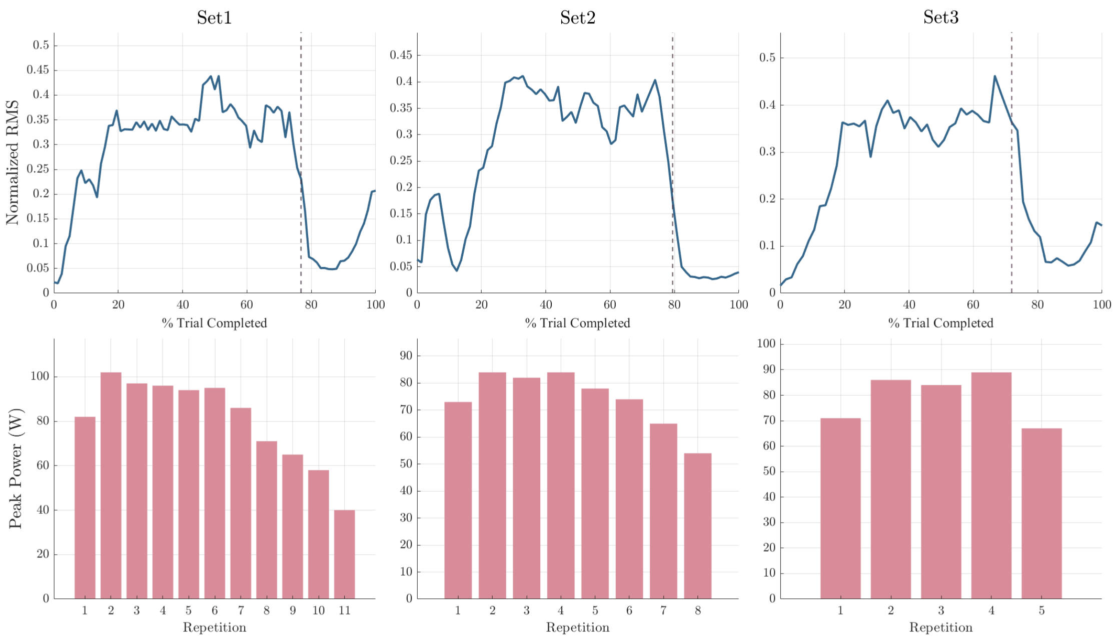

Figure 4.4: Representative MMG RMS trajectories and corresponding power output for participant P08 across three dynamic exercise sets. Top panels show normalized RMS amplitude over time, with vertical dashed lines indicating the change-points identified by the fatigue detection algorithm. Bottom panels display peak power output for each repetition within the corresponding set. In all three sets, RMS generally increases before dropping sharply near the end, aligning with declining power output. This pattern reflects the onset of neuromuscular fatigue and was consistently observed across participants.

Although this figure shows data from a single participant, the overall pattern of increasing RMS followed by a rapid decline, aligned with a gradual then steeper drop in power was consistently observed across participants. This repeated alignment between MMG-derived fatigue detection and mechanical performance degradation supports the physiological validity of the change-point approach and highlights MMG RMS as a sensitive indicator of imminent fatigue.

Figure 4.5 summarizes the timing of fatigue onset for all participants in sets 1, 2, and 3. The boxplots show that the median fatigue onset occurred around the last 15–20% of the set in all three sets (medians 80–85% of trial completion). There is a degree of inter-individual variability, as seen by the interquartile ranges and whiskers in each set: some individuals experienced fatigue very late (near 90–95% of the set), whereas others showed earlier fatigue onsets (around 65–70% through the set). Despite this variability, the group-level consistency is evident in that most participants clustered around a fatigue onset in the final quarter of the exercise duration for each set. There was no strong systematic shift in fatigue onset across the

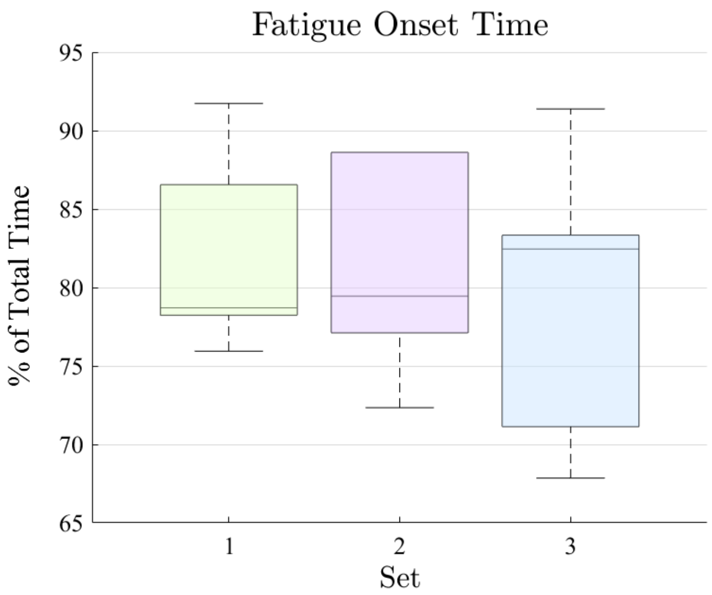

Figure 4.5: Distribution of fatigue onset times across sets based on MMG RMS change-point detection. Boxplots show the percentage of total set duration at which the algorithm detected the onset of fatigue for each set. Median onset times occurred between 78–83% of the trial, with interquartile ranges indicating moderate inter-individual variability. While some participants fatigued earlier or later than others, the majority showed a consistent trend of fatigue onset in the final 20–25% of each set, supporting the robustness of the MMG-based detection method.

three sets and the overlapping spreads indicate that any differences between sets were minor. In summary, the results demonstrate a repeatable pattern: during repetitive dynamic exercise, participants typically reach a fatigue threshold at roughly 80–85% of the set, with slight individual differences in when that threshold is reached, but a consistent group tendency to fatigue near the end of each bout.

4.4 Discussion

This study demonstrates that mechanomyography (MMG) can serve as a reliable and accessible alternative for tracking neuromuscular fatigue during dynamic resistance exercise. By capturing both the amplitude and frequency characteristics of muscle vibrations, MMG revealed consistent, physiologically meaningful patterns that paralleled declines in mechanical output. These findings support growing interest in MMG as a tool for noninvasive fatigue monitoring and offer a foundation for its use in real-time control applications.

Two MMG-derived features were analyzed in this experiment: root mean square (RMS) amplitude and mean power frequency (MPF). RMS reflects the intensity of muscle oscillations and is known to scale with motor unit recruitment and force output. MPF captures the dominant frequency content of those oscillations and reflects the contractile behavior and firing rate of active fibers. In the present study, RMS amplitude typically rose during the early portion of each set, remained elevated through the middle, and then collapsed rapidly near task failure. This "increase-then-decrease" pattern was consistent across participants and sets, and it mirrors classic fatigue responses reported in both isometric and dynamic tasks. Prior work has shown that RMS tends to increase as additional motor units are recruited to sustain force, but drops off sharply once the muscle can no longer maintain contraction quality [84]. This transition was clearly observed in the representative trial shown in Figure 4.4, where MMG RMS remained steady until approximately 80% of the set, after which it dropped sharply in conjunction with power output.

MPF, on the other hand, declined more gradually throughout each set, indicating a progressive slowing of neuromuscular activity. This aligns with previous studies reporting that MMG frequency content decreases with fatigue due to motor unit synchronization and slowing conduction velocity [53, 51]. While MPF was somewhat more variable between individuals, the overall trend toward lower frequencies over time supports its role as an indicator of neuromuscular decline. Previous studies have suggested that MMG RMS tends to correlate more strongly with force or torque loss, while MPF provides complementary but sometimes less stable information [51, 85]. Our results echo this distinction: RMS change was more tightly coupled with performance drops, while MPF captured subtler temporal shifts in contractile behavior.

To quantify the onset of fatigue, a statistical change-point detection algorithm was applied to the MMG RMS curves. This method identified the point at which the signal trend shifted from a stable plateau to a steep decline, interpreted here as the physiological onset of fatigue. Most participants exhibited fatigue onset between 75–85% of set duration, with some inter-individual variability. The ability of this algorithm to consistently detect meaningful transitions in MMG signals highlights its potential utility for real-time fatigue monitoring.

In addition to MMG, this study tracked power output across sets to serve as a mechanical measure of muscle performance. Power was chosen as the primary mechanical outcome rather than force measurements because it reflects not only the magnitude of force production but also the speed of muscle contraction. This is particularly relevant in dynamic resistance exercises where performance depends on both how much force the muscle can generate and how rapidly it can produce that force. Even when force output remains relatively stable, fatigue can manifest as a slowing of contraction speed, indicating increased neuromuscular effort to perform the same movement [86]. By capturing both dimensions, power output provides a more comprehensive measure of muscle function under fatiguing conditions. Power consistently declined over the course of each set, reflecting the muscle's diminishing ability to generate force rapidly. This decline often mirrored changes in MMG RMS, with the two signals diverging sharply near the end of each set, further validating the sensitivity of MMG to functional fatigue.

An important practical implication of these findings is the potential for MMG to serve as a low-cost alternative to expensive equipment like the BeyondPower Voltra, which retails for around $2,000. The consistency between MMG RMS trends and power output suggests that MMG can provide comparable insights into fatigue without the need for complex instrumentation. MMG sensors are lightweight, inexpensive, and easy to integrate into wearable systems, making them especially well-suited for rehabilitation settings where cost and mobility are critical.

Although the analyses presented here were conducted post hoc, the change-point detection method lends itself well to real-time implementation. Because it relies on simple statistical comparisons in rolling windows, it could be integrated into adaptive control schemes or fatigue-aware feedback loops. For example, MMG-based change detection could be used to trigger set termination, modulate exercise intensity, or adjust stimulation levels in assistive devices. As shown in Figure 4.5, while the average fatigue onset occurred around 80% of each set, individual thresholds varied, highlighting the need for personalized, responsive fatigue detection. Future implementations could leverage this algorithm to provide real-time feedback to users or clinicians, enabling smarter, safer training tailored to each individual's physiological capacity.

4.5 Limitations

There were several constraints inherent to this proof-of-concept study. First, the sample comprised only nine healthy, college-aged adults. Their neuromuscular performance, recovery capacity, and movement proficiency likely differ from those of clinical populations, older individuals, or highly trained athletes, limiting generalization across age ranges, health statuses, and training backgrounds.

Second, data collection focused exclusively on the biceps brachii of the non-dominant arm. While that choice helped to maximize signal amplitude and control for dominance-related asymmetries, it overlooks inter-muscle variations in fiber composition, architectural complexity, and recruitment strategies. Consequently, the findings may not fully translate to larger or deeper muscle groups, synergistic muscle interactions, or lower-limb tasks that involve different biomechanical demands.

Third, the experimental tasks were confined to a single, repetitive dynamic movement performed on a motorized cable system. This highly controlled setup allowed for clean signal acquisition but does not reflect the variability and complexity of multi-joint, real-world activities. Additionally, the BeyondPower Voltra's variable resistance profile differs from other training modalities, such as free weights or elastic bands, which may influence neuromuscular responses and signal characteristics.

Finally, the study was acute in nature. It tracked immediate changes in mechanical output and MMG features over a single session but did not examine longer-term adaptations such as strength gains, endurance improvements, neural plasticity, or fatigue-induced muscle damage. These responses could influence MMG patterns differently and warrant longitudinal investigation.

4.6 Future Work

Future research should explore the real-time implementation of the change-point detection algorithm developed in this study. While the current analysis was performed offline, the computational requirements of rolling-window RMS and MPF calculations are modest and well within the capabilities of modern microcontrollers or embedded systems. Implementing real-time detection of fatigue-related changes could enable dynamic adjustments of exercise intensity or provide immediate feedback to users, potentially enhancing the safety and effectiveness of training and rehabilitation programs.

Validation studies under real-time conditions would be essential to confirm the reliability and responsiveness of this approach during live exercise. Additionally, future work should examine whether MMG-based thresholds can be individualized over time, adapting to changes in baseline muscle performance or fatigue resistance. Expanding the study population to include older adults, clinical populations, and athletes could further clarify the generalizability of MMG-based fatigue monitoring. Finally, integration with wearable hardware would move this technology toward practical applications, enabling automated, fatigue-informed exercise dosing in real-world environments.

Beyond isolated resistance movements, future work should also investigate how MMG-based monitoring performs in more complex and coordinated dynamic tasks. Multi-joint exercises and functional tasks introduce greater variability in movement patterns, muscle recruitment strategies, and sensor placement challenges. Evaluating MMG signals in these contexts will be important for understanding their robustness and interpretability under realistic conditions. Success in such tasks would further support MMG's use in applications like rehabilitation progress tracking, occupational health monitoring, and assistive technologies.

4.7 Conclusion

This study demonstrated the viability of mechanomyography as a tool for monitoring neuromuscular fatigue during dynamic resistance exercise. Key MMG features captured physiologically meaningful patterns that aligned with performance declines and fatigue onset across multiple sets. A change-point detection algorithm successfully identified inflection points in MMG RMS signals that corresponded with reductions in mechanical power output, reinforcing the close relationship between muscle output and mechanical oscillations. Together, these findings suggest that MMG provides a cost-effective, portable, and physiologically grounded alternative to traditional fatigue monitoring systems.

Though limited in scope and population, this proof-of-concept work provides a strong foundation for future studies aimed at deploying MMG in real-world settings. With further development, MMG combined with real-time change detection could serve as a valuable tool for personalized, responsive exercise prescription across clinical, athletic, and everyday contexts.

Chapter 5

Case Study: EMG Comparison

5.1 Introduction

Electromyography (EMG) has long been the used as the reference standard for quantifying muscle activity by measuring the electrical events that trigger a contraction. Yet EMG is not without flaws: electrode placement, sweat-induced impedance changes, and electrical stimulation artifacts all complicate both signal acquisition and interpretation. Mechanomyography (MMG), which senses the mechanical vibrations produced as muscle fibers shorten, offers a complementary window into the same physiological process. Because MMG is immune to electrical interference, researchers have begun to explore it as an alternative for muscle activity analysis in a variety of applications.

Many of the signal processing strategies that make EMG useful also translate directly to MMG [87]. The two modalities therefore invite comparison. MMG is still working toward the level of clinical acceptance of that of EMG; demonstrating validity between the two signals strengthens its case. Understanding where the signals diverge can reveal new physiological insights or point to hybrid sensing schemes that may outperform either modality alone.

This chapter reports a direct comparison of simultaneously recorded EMG and MMG data collected from a single participant during a fatiguing grip-hold task. The trial was designed as a validation study of the Curling Artifical Soft ExoskeleTon (CASET), a supernumerary robotic device designed to transfer load from the fingertips to the wrist, thereby reducing grip fatigue and extending hold times. More information on CASET can be found in [88]. The protocol for this validation trial was designed independently, and the dataset was made available only after data collection had concluded. As such, the analysis presented here should be viewed as an opportunistic examination of the electrical and mechanical signals captured during that test. Because the experiment prioritized device validation rather than the characterization of fatigue via mechanomyographic signals, certain design considerations that guided earlier chapters were not implemented here. The findings should thus be interpreted with the CASET validation context in mind.

To isolate natural muscle behavior, the discussion focuses on the unassisted (without CASET) condition. Analysis centers on the flexor digitorum superficialis (FDS) and the extensor carpi radialis (ECR), the primary muscles responsible for finger flexion and wrist extension, respectively. Both muscles are key contributors for generating grip strength and stabilizing the forearm during load-bearing activities [89]. Figure 4.1 highlights their anatomical locations and recommended sensor placement.

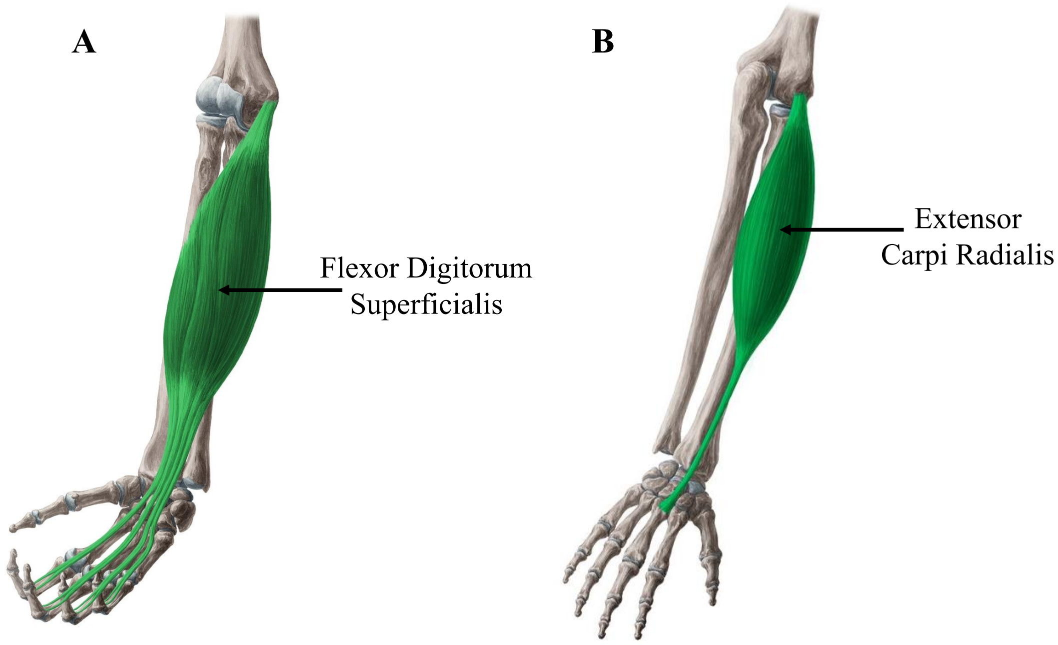

Figure 5.1: Anatomical illustrations of the forearm highlighting the muscles monitored in the study: (A) the flexor digitorum superficialis (FDS), a primary finger-flexor on the anterior forearm, and (B) the extensor carpi radialis (ECR), a principal wrist extensor on the posterolateral forearm [9, 10]. Black arrows indicate the approximate midpoint of each muscle belly where EMG sensors were placed.

5.2 Materials and Methods

5.2.1 Participant

The study protocol was approved by Auburn University's IRB (Protocol STUDY00000267). Ten volunteers completed the broader experiment, however simultaneous EMG and MMG signals were only collected for one participant; the current analysis therefore focuses on that data set. The participant was a healthy 27-year-old male (height: 173.2 cm, weight: 65 kg) with no known neuromuscular impairments. He provided written informed consent and was briefed on all procedures before testing began.

5.2.2 Experimental Protocol

The participant sat upright in a chair and held a pair of 11.3 kg dumbbells in each hand for as long as possible to induce forearm fatigue. Upon failure, the participant was instructed to release the weights. This task was performed twice, both with and without CASET, however the analysis presented in this chapter considers only the unassisted trial. A timer recorded the total hold duration. Figure 5.2 illustrates the experimental setup used for the fatiguing task and highlights EMG sensor placement.

5.2.3 Data Acquisition and Signal Processing

Surface EMG and triaxial accelerometry (IMU) were recorded simultaneously on each forearm with wireless Avanti sensors. The electrodes were centered over the FDS and ECR muscle bellies after standard skin preparation (shave, abrade, isopropyl wipe). Signal acquisition was performed using the EMGWorks Acquisition software, which applied a bandpass filter from 20 to 450 Hz to the EMG signal to remove motion artifacts and high-frequency nouse outside the typical EMG frequency range. The data files were exported as comma-separated values and imported into MATLAB for further analysis. The embedded time-stamps showed two asynchronous sampling rates: the sEMG channels were acquired at 1259 Hz whereas the IMU in each sensor streamed at 148 Hz. It should be noted that ideal MMG signal acquisition would sample at a much higher rate to encompass the 5-100 Hz bandwidth of muscle mechanical

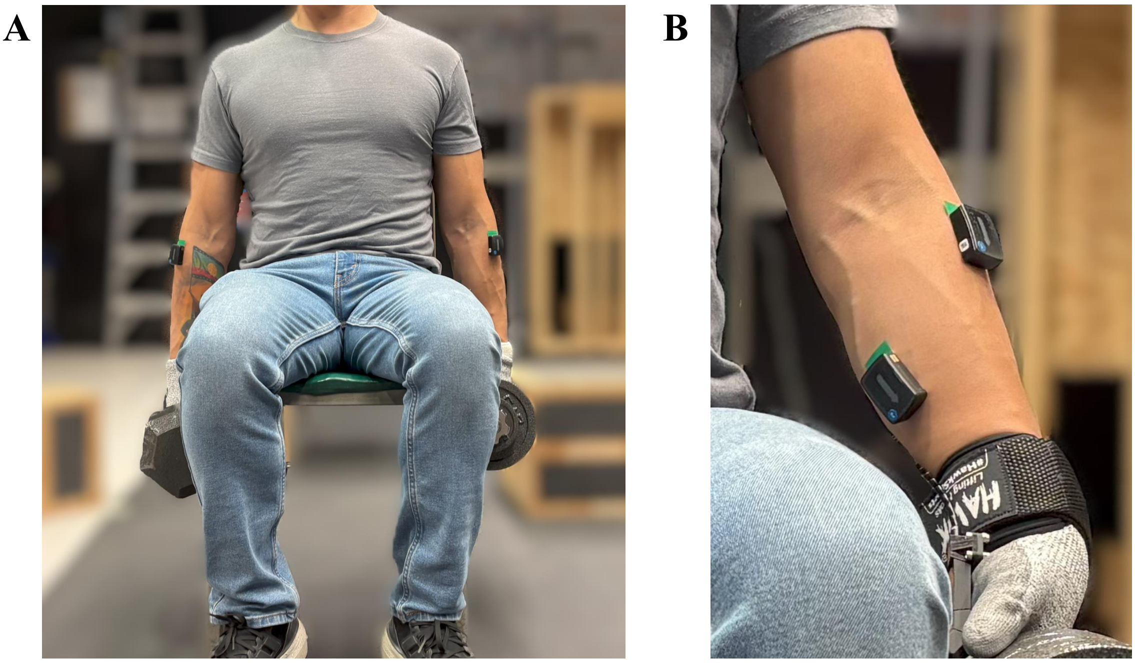

Figure 5.2: Experimental setup and sensor placement for the forearm-fatigue protocol. (A) The participant sat upright with elbows extended and wrists neutral, statically holding 11.3 kg dumbbells in each hand until volitional failure to induce forearm fatigue. (B) Close-up of the left forearm showing the two EMG sensors: the proximal unit is centered over the extensor carpi radialis and the distal unit over the flexor digitorum superficialis.

signals. Though this study used a different sensor and acquisition workflow than discussed in previous experiments, MMG signal processing followed the same pipeline outlined in Chapter 2.

Each accelerometer axis was passed through a 4^{th}-order zero-phase high-pass filter at 5 Hz to remove the constant gravity component and slow postural drift. The magnitude of the acceleration signal was then computed as the Euclidean norm of the three axes. No additional filtering was performed on the EMG signals. Both modalities were segmented into 0.5-s windows. For every window the root-mean-square amplitude (RMS) and mean-power frequency (MPF) were extracted. The mid-point of each segment was converted to a percentage of total task time so that electrical and mechanical curves could be displayed on a common horizontal axis. The RMS and MPF traces were normalized to the mean of the first 10% of segments and smoothed with a three-point moving average to suppress residual jitter [77].

5.3 Results

Over the 129 s unassisted hold, the forearm muscles showed clear signs of fatigue in the EMG recordings, while the MMG signals revealed bursts of mechanical tremor only at later stages. Figure 5.3 and Figure 5.4 summarize the feature trends for the FDS and ECR muscles, respectively, with the left (non-dominant) limb on the left side of each figure and the right (dominant) limb on the right side. In each plot, EMG-derived features are depicted alongside MMG-derived features across the normalized task duration.

In the FDS, EMG-RMS increased over the duration of the hold task in both limbs, accompanied by a progressive decline in EMG-MPF. The rise in RMS was more pronounced on the non-dominant side, which also exhibited a steeper drop in spectral content. MMG signals displayed delayed but distinct bursts in magnitude near the latter stages of the trial, particularly

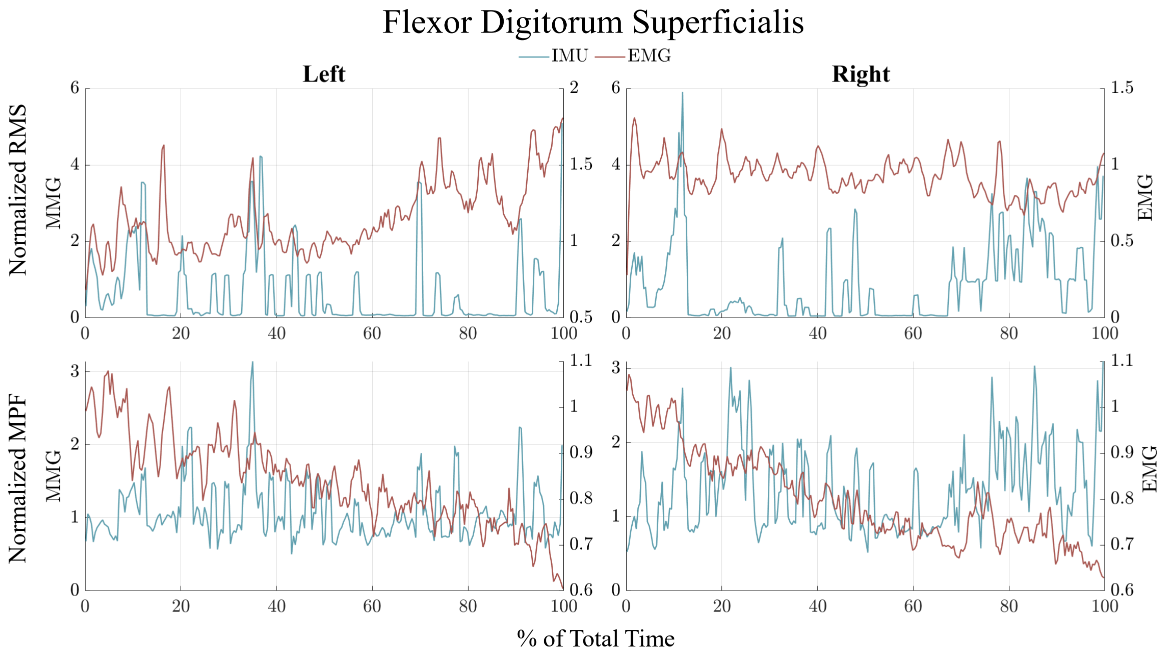

Figure 5.3: Each panel overlays acceleration magnitude (MMG, blue, left ordinate) and surface-EMG (EMG, orange, right ordinate). Top row: normalized RMS; bottom row: normalized MPF. The left column represents the non-dominant forearm, the right column the dominant forearm. In both forearms EMG shows a continuous rise in RMS accompanied by a compression of MPF, indicating progressive recruitment of fast-twitch motor units. Large-amplitude MMG bursts appear only after electrical fatigue is well established (60% of trial time in the non-dominant limb, 45% in the dominant limb), demonstrating that overt tremor lags behind its electrical precursors.

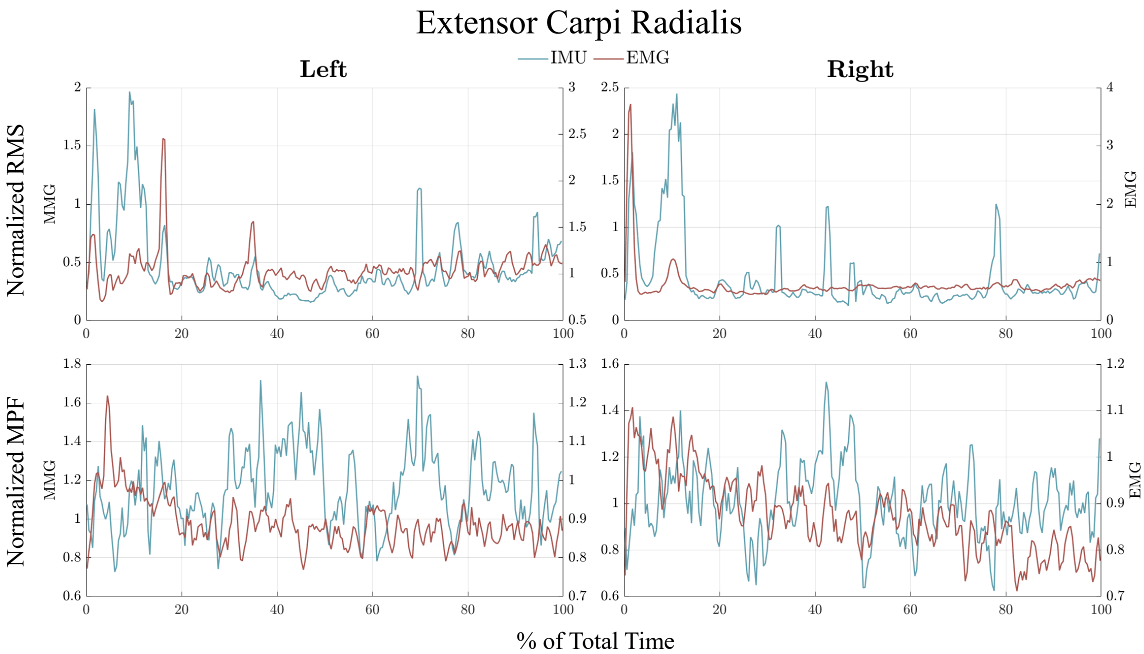

Figure 5.4: Plot layout and color coding are identical to Figure 5.3. Only brief, isolated MMG amplitude bursts are visible and both EMG metrics remain within ±20% of baseline, confirming that ECR served chiefly as a low-fatigue wrist stabilizer during the grip-hold. Dashed grid lines mark 20% increments of total trial time

on the non-dominant side, with corresponding transient elevations in MMG-MPF. These bursts occurred after most of the EMG amplitude increase had already taken place.

The ECR exhibited comparatively stable behavior. EMG-RMS and EMG-MPF remained close to baseline throughout the trial, with only modest fluctuations. MMG metrics also showed little deviation: RMS stayed near initial values, and MPF demonstrated no consistent trend over time. No sustained tremor-like bursts were observed in the ECR MMG data.

Despite symmetrical external loading, side-to-side differences emerged. The dominant FDS began at a higher EMG amplitude but showed a smaller overall gain, while the non-dominant side displayed a larger relative increase in EMG-RMS and more prominent MMG bursts near the end of the task

5.4 Discussion

The fatigue behaviors observed in the flexor digitorum superficialis (FDS) and extensor carpi radialis (ECR) can be explained in large part by their contrasting fiber-type compositions. The

FDS is a muscle with a mixed fiber-type distribution, containing an approximately even distribution of both fatigue-resistant slow-twitch fibers and fast-fatiguing fast-twitch fibers. In sustained contractions at moderate force levels, the type I fibers of the FDS can maintain force for a considerable duration using oxidative (aerobic) metabolism, delaying fatigue. As those fibers gradually tire or as more force is needed, the larger type II fibers are progressively recruited to uphold the force, but these fibers rely on glycolytic metabolism and fatigue more rapidly [90]. The result is a progressive recruitment pattern: early in the task, mostly slow-twitch units are active (low EMG amplitude, high firing frequencies giving a higher EMG MPF). Over time, more and more fast-twitch units are activated to compensate for weakening slow units, causing the EMG amplitude to climb and the overall EMG power spectrum to shift lower (since the newly recruited larger units tend to have lower firing rates and the fatigue process slows all firing rates). This explains the steady increase in EMG RMS and the concurrent drop in EMG MPF we saw in the FDS. Importantly, the muscle did not start to produce high-amplitude MMG vibrations until a critical amount of those fast-twitch units were active and beginning to fail in maintaining smooth force. At that point, late in the contraction, the muscle's contractions became more unfused and erratic, manifesting as tremor bursts in the MMG signal. In simpler terms, the FDS's electrical fatigue signs (indicating recruitment of fast units and slowing of firing rates) were evident well before the mechanical signs (tremor), because the muscle could compensate for fatigue by recruitment for a long period. Only when it had recruited most available fibers did the contractions become jerky. This pattern aligns with the idea that MMG frequency content often remains stable through much of a sustained contraction and only changes markedly when there is unfused, large-unit activity.

The extensor carpi radialis, on the other hand, is a predominantly fast-twitch muscle in humans designed more for quick, powerful wrist movements than for endurance [91]. Being a postural stabilizer in this task, it wasn't heavily loaded, which meant many of its high-threshold motor units were likely never even recruited during the hold. In this isometric hold, the ECR's job was mainly to counterbalance the flexion moment at the wrist, which required relatively low force. Thus, the ECR could carry out this role by activating only a small portion of its fibers and never needed to tap into the bulk of its fast-twitch reserve. Consequently, the EMG of ECR stayed low-level and didn't show a major fatigue trend as the muscle was operating well below its fatigue threshold. Correspondingly, the MMG signal did not exhibit significant tremor because the ECR's contractions remained smooth and largely fused; there was no large-scale recruitment of fast units to cause shaking [92]. If the task had required stronger wrist extensor effort, we might have seen the ECR engage more motor units and eventually show fatigue signs. Notably, comparative studies have found that the extensor muscles like ECR are indeed primarily utilized when high force or rapid movements are needed, whereas for static low-force tasks they contribute minimally [90]. This explains why for this static hold the ECR was mostly stable; its physiology is geared toward intense bursts, not long holds.

The side-to-side (dominant vs nondominant) differences observed in the FDS can also be interpreted through a fiber-type and training lens. The muscles of the dominant arm are typically stronger and often exhibit adaptations from frequent use. Some studies even suggest that lifelong preferential use can alter fiber-type composition or motor unit behavior in the dominant limb [93]. It is possible that the dominant FDS had a greater proportion of larger motor units (or at least was conditioned to use them more readily), resulting in an initially higher EMG output and a tendency to rely on those units early. Those large units would fatigue sooner, causing mechanical instability to appear relatively early as well. The nondominant FDS, perhaps with relatively more fatigue-resistant fibers or simply a different recruitment pattern, showed a slower buildup of fatigue signs but ultimately had to recruit heavily by the end, at which point it too showed tremor. This difference underlines how individual muscle composition and neural strategy can modulate the fatigue process, an interesting topic for further study.

Overall, these findings reinforce two practical points about using EMG and MMG for fatigue monitoring. First, EMG-based metrics provide an early warning of fatigue. Long before a muscle starts trembling or obviously failing, its EMG amplitude and frequency characteristics are shifting in a predictable way. This gives a window of opportunity to detect fatigue developing and potentially intervene (e.g., reduce load, change technique, or activate an assistive device) before performance is visibly degraded. Second, MMG signals can identify when fatigue has progressed to the point of affecting mechanical performance. The pronounced muscle tremor picked up by the accelerometer indicates that the muscle can no longer maintain smooth force output, which is highly relevant for functional tasks, as tremor can impair precision and increase injury risk. In the field of rehabilitation, knowing when such tremor begins could help set safe therapy intensity levels.

5.5 Limitations

Several factors constrain broader interpretations of the findings of the current case study. First and most obvious is the sample size: data were collected from a single 27-year-old male. Individual muscle activation patterns and fatigue thresholds may vary substantially across people; hence the results may not generalize to other ages, sexes, or training backgrounds without further replication.

Second, the experimental task was a sustained isometric grip-hold. Static contractions elicit different neuromuscular dynamics than other cyclic or functional movements, so the relative behavior of EMG and MMG observed here may not translate to dynamic tasks. Extending the protocol to include a broader repertoire of movements would provide a more complete understanding of the strengths and weaknesses of each modality.

Third, only two forearm muscle groups were analyzed. These muscles were chosen because they are primary contributors to grip, yet they do not capture synergistic or antagonistic activity in the intrinsic hand muscles, wrist stabilizers, or proximal arm segments that also influence fatigue. Recording from a more comprehensive set of muscles would clarify whether the EMG-MMG relationship observed is specific to distal forearm musculature or holds throughout the kinetic chain.

Additionally, the hardware used in this experiment differed from that used in earlier chapters. The Delsys sensors weighed approximately 15 g, exceeding the $\leq$ 13 g guideline for accelerometers intended to track muscle vibrations. This extra inertia may have damped the upper end of the 5-100 Hz band where much of the mechanical energy resides, altering both amplitude and spectral content. Moreover, as mentioned, the IMU sampling rate (148 Hz) was relatively low. Ideally, to capture up to 100 Hz of vibration content without aliasing, one would sample at 200 Hz or more. Using a higher sampling rate might reveal additional details in the MMG spectrum that were missed here.

Lastly, because the intended purpose of the experiment was for device validation (CASET), certain optimizations that one would include in a dedicated EMG–MMG fatigue study were not present. For example, the load was not standardized to each individual's maximum and the focus on device assistance in the larger study meant that the unassisted condition was just one part of the protocol. All these factors mean the current findings should be viewed as preliminary and specific to the conditions tested, rather than definitive general truths

5.6 Future Work

Looking ahead, the most immediate priority is to move from this single subject proof-of-concept to a statistically powered study. Recruiting a larger, demographically diverse subject pool varying in age, sex, and training status will clarify how robust the EMG-MMG relationships are to inter-individual differences. The movement repertoire should also be expanded. Incorporating dynamic tasks, such as tool manipulation or activities of daily living, will test whether the trends observed in a sustained isometric grip persist when joint kinematics become more complex. Furthermore, translating the protocol to clinical populations would test the practical value of an EMG-MMG hybrid approach. Demonstrating tangible benefits, like prolonged work times or reduced injury rates using an EMG-MMG feedback system, would be a compelling outcome of future research.

Hardware considerations are equally important. Future studies should adopt sub-13 g MEMS accelerometers with bandwidths exceeding 200 Hz and synchronize both EMG and MMG signal acquisition at comparable sample rates. Lightweight sensor housings will reduce inertial damping and higher-rate acquisition will improve spectral resolution, especially for fast-fatiguing muscles like the ECR. Multimodal data fusion techniques also merit exploration. Machine learning models that analyze EMG, MMG, and basic kinematics could learn personalized fatigue signatures and predict impending grip failure more accurately than any single signal.

5.7 Conclusion

In this case study, we directly compared electrical and mechanical signals from forearm muscles during a prolonged, fatiguing grip hold. The analysis revealed that EMG provides a leading indicator of muscle fatigue, which occurred before mechanical tremor, specifically in the flexor digitorum superficialis. Only later, as fatigue advanced, did the MMG signal show bursts of high-amplitude oscillations accompanied by shifts to higher vibration frequencies, signaling that the muscle contractions had become unsteady. The extensor carpi radialis muscle, being less taxed, showed minimal changes in either signal, underscoring its role as a stabilizer with higher fatigue resistance under the given load.

The key takeaway is that EMG and MMG offer complementary, time-staggered information about the muscle's state. EMG changes gradually and can warn of diminishing endurance proactively, while MMG captures the moment when fatigue finally manifests as loss of force control (which is critical for functional failure). In practical applications, this suggests a layered monitoring approach: one can use EMG to track accumulating fatigue and perhaps adjust workload or provide assistance before the muscle starts to shake, and use MMG to confirm when fatigue has reached a point of functional degradation, indicating that an immediate intervention is required. Such an approach could improve both safety and performance in settings ranging from sports training to physical rehabilitation. This case study, though limited, lays the groundwork for future research and development in this direction. It demonstrates in a real scenario how the two modalities can be recorded together and how their signals can be interpreted in tandem. As sensing technology and analytical techniques advance, the hope is that real-time EMG–MMG monitoring could be deployed in everyday tools to extend human endurance and prevent injury. The present findings provide an encouraging proof-of-concept for that vision, showing that MMG can add value to what EMG tells us about muscle fatigue.

Chapter 6

Conclusion

Neurorehabilitation research is an ongoing effort driven by the need for effective interventions that not only restore function but also provide objective, quantifiable measures of recovery and progress. A critical component of this effort is the development of reliable feedback systems capable of guiding personalized and adaptive rehabilitation routines [94]. Such systems have the potential to optimize therapy for individuals, reduce clinician burden, and ultimately improve functional outcomes.

This thesis explored the potential of mechanomyography (MMG) as a practical and cost-effective tool for monitoring mucle fatigue during both static and dynamic muscle actions. Through a series of experimental studies, it was demonstrated that MMG metrics reliable reflected fatigue related changes in muscle behavior. In static contraction tasks, clear trends were observed in MMG amplitude and frequency characteristics as fatigue developed, suggesting the technique's sensitivity to neuromuscular decline. In dynamic tasks, MMG similarly captured fatigue related changes despite the additional complexities of movement and varying contraction velocities, underscoring its robustness in more functionally relevant activities.

Beyond validating MMG as a fatigue monitoring tool, the research proposed a thresholding approach to detect fatigue onset, which could readily be integrated into real-time control systems. Such integration would enable adaptive modulation of therapy parameters to sustain effective muscle contractions and delay task failure. This has significant implications for extending exercise duration, reducing patient fatigue, and enhancing therapeutic outcomes.

6.1 Future Work

Future work could build upon the research presented here in several promising avenues. A primary direction involves embedding the proposed fatigue thresholding framework into real-time feedback control algorithms for functional electrical stimulation applications. By dynamically adjusting stimulation parameters in response to MMG-based fatigue indicators, such systems could prolong the duration of effective muscle contractions and reduce premature task failure. Implementing these fatigue aware adjustments could be particularly valuable for individuals with neurological conditions, who often struggle with muscle endurance during repetitive rehabilitation tasks.

Another compelling area for future development lies in hybrid control approaches that combine FES with wearable robotic assistance. Rehabilitation robotics has made significant strides in recent years, offering precise, programmable movements and opportunities for intensive therapy. Yet, many studies have found that robotic interventions alone often yield outcomes comparable to traditional therapy, suggesting room for improvement in their clinical impact [95]. Integrating MMG-based fatigue monitoring into hybrid systems could optimize how assistance is shared between robotic actuators and electrically stimulated muscle contractions. By intelligently alternating the mechanical load between the robot and the patient's own muscles, such systems might reduce power demands on robotic hardware while promoting active patient engagement, a key factor in driving neuroplastic recovery [].

Beyond control applications, future research should also investigate the use of MMG for individualized rehabilitation profiling. Because fatigue responses vary between individuals, MMG could help clinicians tailor exercise intensity, duration and progression to each patient's unique neuromuscular capacity. Developing algorithms that characterize an individual's fatigue thresholds and patterns over time could support personalized therapy plans and more precise tracking of recovery progress.

Further research should also focus on the continued development and optimization of MMG sensor technology. The sensor used in this thesis was a wired system, which, while effective in a laboratory environment, can be cumbersome and limit freedom of movement, particularly in dynamic tasks or home-based rehabilitation scenarios. Transitioning to wireless MMG sensors would greatly enhance usability and comfort. Developing compact, low-power, wireless MMG devices that maintain high signal fidelity is a crucial step toward enabling seamless integration into wearable systems and daily-life monitoring applications.

Finally, future work could examine the integration of MMG with other sensing modalities, such as force sensors, ultrasound imaging, or other physiological signals like heart rate variability. Multimodal systems could provide a more holistic picture of neuromuscular performance, fatigue, and overall physical health. Beyond simply improving monitoring accuracy, such integrated systems hold the potential to yield deeper insights into the underlying mechanisms of motor recovery, neuroplasticity, and motor learning processes in both healthy and neurologically impaired populations. Understanding these mechanisms could, in turn, inform the design of more effective rehabilitation protocols and guide therapeutic decision making in a truly personalized way.

Collectively, these directions highlight the considerable potential for MMG not only as a research tool but as a practical component of advanced neurorehabilitation systems. Expanding this work could help transform rehabilitation from largely predetermined protocols into personalized, responsive interventions that adapt in real time to each patient's needs and capabilities.

6.2 Conclusion

In conclusion, the studies presented in this thesis highlight the utility of mechanomyography as a reliable, versatile, and cost-effective tool for quantifying muscle fatigue. The insights gained from static and dynamic testing, as well as comparative analysis with EMG, provide a strong foundation for future integration into rehabilitation systems. Ultimately, incorporating MMG into real-time control strategies holds significant potential for enhancing neurorehabilitation by enabling precise, adaptive, and patient-specific therapeutic interventions.

Appendices

A.1 Python Data Acquisition Script

The following script was used to collect and log triaxial accelerometer data from the ADXL367 using a Raspberry Pi Pico.

```
import serial
import csv
import time
import numpy as np
import matplotlib.pyplot as plt

# Configure Serial Port
ser = serial.Serial('COM3', 115200, timeout=1)
plt.ion()
csv_filename = "filename.csv"
buffer_size = 100
data_buffer = []
start_time = None
last_sample = None
replacement_sample = 0
partial_data = ""

baseline_rms_z = None
percent_change_list = []
fatigue_detected = False
```

```
threshold = -10

sample_rate = 400
time_per_sample = 1 / sample_rate
window_size = 2000

sample_numbers = []
time_data = []
x_data = []
y_data = []
z_data = []

with open(csv_filename, mode="w", newline="") as file:
    writer = csv.writer(file)
    writer.writerow(["Sample", "Time", "X", "Y", "Z"])
    try:
        while True:
            raw_data = ser.read(ser.in_waiting or 1).decode('utf-8', errors='ignore')
            partial_data += raw_data
            lines = partial_data.split("\n")
            if raw_data[-1] != "\n":
                partial_data = lines.pop()
            else:
                partial_data = ""

            for line in lines[:-1]:
                line = line.strip()
                if not line.startswith("<") or not line.endswith(">"):
```

```python
                print(f"Skipping malformed line: {line}")
                with open("malformed_lines.log", "a") as log_file:
                    log_file.write(line + "\n")
                continue

            line = line[1:-1]
            values = line.split(",")
            if len(values) != 4:
                print(f"Skipping malformed line: {line}")
                continue

            try:
                sample = int(values[0])
                x, y, z = map(float, values[1:])
                if last_sample is not None and sample < last_sample:
                    print(f"WARNING: Reset detected at sample {sample}, last_sample: {last_sample}. Adjusting...")
                    sample = last_sample + 1

                replacement_sample += 1
                time_in_seconds = replacement_sample / 400
                data_buffer.append([replacement_sample, time_in_seconds, x, y, z])
                last_sample = sample

                if len(data_buffer) >= buffer_size:
                    writer.writerows(data_buffer)
```

```
                        data_buffer.clear()
                except ValueError:
                    print(f"Skipping invalid data: {values}")
    except KeyboardInterrupt:
        print("Stopping Data Collection...")
    finally:
        ser.close()
```

Listing 1: Python script for serial MMG data acquisition

A.2 MATLAB Processing Script

The following MATLAB script was used to process the raw MMG data collected during the experimental trials. It converts the Z-axis accelerometer data from gravitational units (g) to SI units (m/s^2), applies a 4^{th}-order Butterworth bandpass filter, and computes temporal (RMS) and spectral (MPF) features over a sliding window for fatigue analysis.

```
% MMG_FeatureExtraction.m
% This script processes raw MMG data from CSV:
% - Converts g to m/s^2
% - Applies 4th order bandpass Butterworth filter
% - Calculates RMS and MPF over sliding windows

clear; clc;

% ---- Parameters ----
filename = 'filename.csv';      % Your CSV file name
fs = 400;                       % Sampling frequency in Hz
g_to_ms2 = 9.80665;             % Conversion from g to m/s^2
window_sec = 0.5;               % Window size in seconds
window_size = round(fs * window_sec);
overlap = round(0.5 * window_size);  % 50% overlap

% ---- Load Data ----
data = readtable(filename);
time = data.Time;
z_raw = data.Z * g_to_ms2;      % Convert Z-axis from g to m/s^2

% ---- Bandpass Filter ----
[b, a] = butter(4, [5 100] / (fs / 2), 'bandpass');
z_filt = filtfilt(b, a, z_raw);
```

```

% ---- Feature Extraction ----
num_samples = length(z_filt);
rms_vals = [];
mpf_vals = [];
time_centers = [];

for i = 1:overlap:(num_samples - window_size)
    segment = z_filt(i:i + window_size - 1);

    rms_val = sqrt(mean(segment.^2));
    rms_vals(end+1) = rms_val;

    xdft = fft(segment);
    xdft = xdft(1:floor(length(xdft)/2));
    psd = (1/length(segment)) * abs(xdft).^2;
    freqs = linspace(0, fs/2, length(psd));
    mpf = sum(freqs .* psd') / sum(psd);
    mpf_vals(end+1) = mpf;

    time_centers(end+1) = time(i + floor(window_size/2));
end
```

Listing 2: MATLAB script for MMG feature extraction and analysis

References

[1] V. L. Feigin, T. Vos, E. Nichols, M. O. Owolabi, W. M. Carroll, M. Dichgans, G. Deuschl, P. Parmar, M. Brainin, and C. Murray, "The global burden of neurological disorders: translating evidence into policy," *The Lancet. Neurology*, vol. 19, no. 3, pp. 255–265, Mar. 2020. [Online]. Available: https://www.ncbi.nlm.nih.gov/pmc/articles/PMC9945815/

[2] A. Lalime, "Motor Unit Recruitment & Biofeedback in Rehabilitation," Apr. 2020. [Online]. Available: https://www.mtrigger.com/motor-unit-recruitment-biofeedback-in-rehabilitation/

[3] "System 4 Pro™." [Online]. Available: https://biodexrehab.com/products/system-4-pro/

[4] "Jamar Hand Strength Evaluation Dynamometer — Mountainside Medical." [Online]. Available: https://www.mountainside-medical.com/products/jamar-hand-dynamometer

[5] A. Pietroski, Y. Zhou, J. Kasto, C. Obinero, K. Zhu, M. Mazeh, C. Chen, S. Muh, A. Pietroski, Y. Zhou, J. Kasto, C. Obinero, K. Zhu, M. Mazeh, C. Chen, and S. Muh, "Surface Electromyography Reveals Middle Deltoid as the Functionally Dominant Shoulder Muscle After Reverse Total Shoulder Arthroplasty," *Cureus*, vol. 17, Mar. 2025, publisher: Cureus. [Online]. Available: https://www.cureus.com/articles/206668-surface-electromyography-reveals-middle-deltoid-as-the-functionally-dominant-shoulder-musc

[6] Analog Devices, "Adxl367: Micropower, 3-axis, mems accelerometer," 2024, accessed: 2025-07-29. [Online]. Available: https://www.analog.com/en/products/adxl367.html

[7] "Voltra I." [Online]. Available: https://www.xeniosusa.com/en/voltra-i.html

[8] "Beyond+ App | Unlock Your Training Insight | Track Real-Time Data." [Online]. Available: https://www.beyond-power.com/pages/beyond-plus

[9] "Flexor digitorum superficialis muscle." [Online]. Available: https://www.kenhub.com/en/library/anatomy/flexor-digitorum-superficialis-muscle

[10] "Extensor carpi radialis brevis muscle." [Online]. Available: https://www.kenhub.com/en/library/anatomy/extensor-carpi-radialis-brevis-muscle

[11] T. L. Neurology, "Sex, gender, and the cost of neurological disorders," *The Lancet Neurology*, vol. 22, no. 5, p. 367, May 2023, publisher: Elsevier. [Online]. Available: https://www.thelancet.com/journals/laneur/article/PIIS1474-4422(23)00120-5/fulltext

[12] P. Zarek, C. Ruttinger, D. Armstrong, R. Chakrabarti, D. R. Hess, T. J. Manal, and T. M. Dall, "Current and Projected Future Supply and Demand for Physical Therapists From 2022 to 2037: A New Approach Using Microsimulation," *Physical Therapy*, vol. 105, no. 3, p. pzaf014, Mar. 2025. [Online]. Available: https://doi.org/10.1093/ptj/pzaf014

[13] M. Maier, B. R. Ballester, and P. F. M. J. Verschure, "Principles of Neurorehabilitation After Stroke Based on Motor Learning and Brain Plasticity Mechanisms," *Frontiers in Systems Neuroscience*, vol. 13, Dec. 2019, publisher: Frontiers. [Online]. Available: https://www.frontiersin.org/journals/systems-neuroscience/articles/10.3389/fnsys.2019.00074/full

[14] B. E. Fisher and K. J. Sullivan, "Activity-dependent factors affecting poststroke functional outcomes," *Topics in Stroke Rehabilitation*, vol. 8, no. 3, pp. 31–44, 2001.

[15] C. E. Lang, J. R. MacDonald, D. S. Reisman, L. Boyd, T. J. Kimberley, S. M. Schindler-Ivens, T. G. Hornby, S. A. Ross, and P. L. Scheets, "Observation of amounts of movement practice provided during stroke rehabilitation," *Archives of physical medicine and rehabilitation*, vol. 90, no. 10, pp. 1692–1698, Oct. 2009. [Online]. Available: https://www.ncbi.nlm.nih.gov/pmc/articles/PMC3008558/

[16] L. Wu and H. Jin, "A systematic review of post-stroke fatigue measurement scale based on COSMIN guidelines," *Frontiers in Neurology*, vol. 15, Sep. 2024, publisher: Frontiers Media SA. [Online]. Available: https://www.frontiersin.org/articles/10.3389/fneur.2024.1411472/full

[17] O. K. Sujith, "Functional electrical stimulation in neurological disorders," *European Journal of Neurology*, vol. 15, no. 5, pp. 437–444, 2008, _eprint: https://onlinelibrary.wiley.com/doi/pdf/10.1111/j.1468-1331.2008.02127.x. [Online]. Available: https://onlinelibrary.wiley.com/doi/abs/10.1111/j.1468-1331.2008.02127.x

[18] C.-Y. Fang, A. S.-Y. Lien, J.-L. Tsai, H.-C. Yang, H.-L. Chan, R.-S. Chen, and Y.-J. Chang, "The Effect and Dose-Response of Functional Electrical Stimulation Cycling Training on Spasticity in Individuals With Spinal Cord Injury: A Systematic Review With Meta-Analysis," *Frontiers in Physiology*, vol. 12, Nov. 2021, publisher: Frontiers. [Online]. Available: https://www.frontiersin.org/journals/physiology/articles/10.3389/fphys.2021.756200/full

[19] C. S. Bickel, C. M. Gregory, and J. C. Dean, "Motor unit recruitment during neuromuscular electrical stimulation: a critical appraisal," *European Journal of Applied Physiology*, vol. 111, no. 10, pp. 2399–2407, Oct. 2011. [Online]. Available: https://doi.org/10.1007/s00421-011-2128-4

[20] R. M. Enoka and J. Duchateau, "Muscle fatigue: what, why and how it influences muscle function," *The Journal of Physiology*, vol. 586, no. 1, pp. 11–23, 2008, _eprint: https://physoc.onlinelibrary.wiley.com/doi/pdf/10.1113/jphysiol.2007.139477. [Online]. Available: https://onlinelibrary.wiley.com/doi/abs/10.1113/jphysiol.2007.139477

[21] W. Senn, K. Wyler, H. Clamann, J. Kleinle, H.-R. Lüscher, and L. Müller, "Size principle and information theory," *Biological Cybernetics*, vol. 76, no. 1, pp. 11–22, Jan. 1997. [Online]. Available: https://doi.org/10.1007/s004220050317

[22] M. O. Ibitoye, N. A. Hamzaid, N. Hasnan, A. K. A. Wahab, and G. M. Davis, “Strategies for Rapid Muscle Fatigue Reduction during FES Exercise in Individuals with Spinal Cord Injury: A Systematic Review,” *PLOS ONE*, vol. 11, no. 2, p. e0149024, Feb. 2016, publisher: Public Library of Science. [Online]. Available: https://journals.plos.org/plosone/article?id=10.1371/journal.pone.0149024

[23] M. K. I. Ahmad, A. U. Shamsudin, Z. A. Soomro, R. Abdul Rahim, B. S. K. Kader Ibrahim, and M. S. Huq, “Closed-loop Functional Electrical Stimulation (FES) – cycling rehabilitation with phase control Fuzzy Logic for fatigue reduction control strategies for stroke patients,” *SINERGI*, vol. 28, no. 1, p. 63, Dec. 2023, publisher: Universitas Mercu Buana. [Online]. Available: https://publikasi.mercubuana.ac.id/index.php/sinergi/article/view/21231

[24] E. T. Hedge, C. A. Patterson, C. J. Mastrandrea, V. Sonjak, G. Hajj-Boutros, A. Faust, J. A. Morais, and R. L. Hughson, “Implementation of exercise countermeasures during spaceflight and microgravity analogue studies: Developing countermeasure protocols for bedrest in older adults (BROA),” *Frontiers in Physiology*, vol. 13, Aug. 2022, publisher: Frontiers. [Online]. Available: https://www.frontiersin.org/journals/physiology/articles/10.3389/fphys.2022.928313/full

[25] A. Van Ombergen, A. Demertzi, E. Tomilovskaya, B. Jeurissen, J. Sijbers, I. B. Kozlovskaya, P. M. Parizel, P. H. Van de Heyning, S. Sunaert, S. Laureys, and F. L. Wuyts, “The effect of spaceflight and microgravity on the human brain,” *Journal of Neurology*, vol. 264, no. 1, pp. 18–22, Oct. 2017. [Online]. Available: https://doi.org/10.1007/s00415-017-8427-x

[26] B. A. S. Shepherd, M. E. Guilliams, and T. Taddeo, “Rehabilitation after International Space Station Flights.”

[27] A. Wani, B. Prabhakar, and P. Shende, “Strategic Aspects of Space Medicine: A Journey from Conventional to Futuristic Requisites,” *Space: Science & Technology*, vol. 4, p.

0123, Jun. 2024, publisher: American Association for the Advancement of Science. [Online]. Available: https://spj.science.org/doi/10.34133/space.0123

[28] G. a. V. Borg, "Psychophysical bases of perceived exertion," *Medicine & Science in Sports & Exercise*, vol. 14, no. 5, p. 377, 1982. [Online]. Available: https://journals.lww.com/acsm-msse/abstract/1982/05000/psychophysical_bases_of_perceived_exertion.12.aspx

[29] J. Scherr, B. Wolfarth, J. W. Christle, A. Pressler, S. Wagenpfeil, and M. Halle, "Associations between Borg's rating of perceived exertion and physiological measures of exercise intensity," *European Journal of Applied Physiology*, vol. 113, no. 1, pp. 147–155, Jan. 2013. [Online]. Available: https://doi.org/10.1007/s00421-012-2421-x

[30] H. Zhao, D. Seo, and J. Okada, "Validity of using perceived exertion to assess muscle fatigue during back squat exercise," *BMC Sports Science, Medicine and Rehabilitation*, vol. 15, no. 1, p. 14, Feb. 2023. [Online]. Available: https://doi.org/10.1186/s13102-023-00620-8

[31] J. D. Fisk, P. G. Ritvo, L. Ross, D. A. Haase, T. J. Marrie, and W. F. Schlech, "Measuring the Functional Impact of Fatigue: Initial Validation of the Fatigue Impact Scale," *Clinical Infectious Diseases*, vol. 18, no. Supplement_1, pp. S79–S83, Jan. 1994. [Online]. Available: https://doi.org/10.1093/clinids/18.Supplement_1.S79

[32] Nordin, C. Taft, Lundgren-Nilsson, and A. Dencker, "Minimal important differences for fatigue patient reported outcome measures—a systematic review," *BMC Medical Research Methodology*, vol. 16, no. 1, p. 62, May 2016. [Online]. Available: https://doi.org/10.1186/s12874-016-0167-6

[33] J.-j. Wan, Z. Qin, P.-y. Wang, Y. Sun, and X. Liu, "Muscle fatigue: general understanding and treatment," *Experimental & Molecular Medicine*, vol. 49, no. 10, p. e384, Oct. 2017. [Online]. Available: https://www.ncbi.nlm.nih.gov/pmc/articles/PMC5668469/

[34] D. C. Petian-Alonso, C. S. B. Franco, E. J. Martins, K. L. T. Cruz, R. de Fátima Carreira Moreira Padovez, and A. C. Mattiello-Sverzut, "Instruments and Parameters for

Evaluating Upper Limb Motor Fatigability in Individuals with Neuromuscular Diseases: Systematic Review," *Acta Neurologica Scandinavica*, vol. 2023, no. 1, p. 8373917, 2023, _eprint: https://onlinelibrary.wiley.com/doi/pdf/10.1155/2023/8373917. [Online]. Available: https://onlinelibrary.wiley.com/doi/abs/10.1155/2023/8373917

[35] T. Silva-Santos, R. S. Guerra, R. Valdiviesso, and T. F. Amaral, "Hand Grip Force–Time Curve Indicators Evaluated by Dynamometer: A Systematic Review," *Nutrients*, vol. 16, no. 12, p. 1951, Jun. 2024. [Online]. Available: https://www.ncbi.nlm.nih.gov/pmc/articles/PMC11206825/

[36] S. Kumar, "Localized muscle fatigue: review of three experiments," *Brazilian Journal of Physical Therapy*, vol. 10, pp. 9–28, 2006, publisher: Associação Brasileira de Pesquisa e Pós-Graduação em Fisioterapia. [Online]. Available: https://www.scielo.br/j/rbfis/a/HQQCLtj4jhWXNxZB6Y6mLkn/?lang=en

[37] R. Merletti, A. Rainoldi, and D. Farina, "Surface Electromyography for Noninvasive Characterization of Muscle," *Exercise and Sport Sciences Reviews*, vol. 29, no. 1, p. 20, Jan. 2001. [Online]. Available: https://journals.lww.com/acsm-essr/fulltext/2001/01000/surface_electromyography_for_noninvasive.5.aspx

[38] J. Sun, G. Liu, Y. Sun, K. Lin, Z. Zhou, and J. Cai, "Application of Surface Electromyography in Exercise Fatigue: A Review," *Frontiers in Systems Neuroscience*, vol. 16, Aug. 2022, publisher: Frontiers. [Online]. Available: https://www.frontiersin.org/journals/systems-neuroscience/articles/10.3389/fnsys.2022.893275/full

[39] M. A. M. Bandpei, N. Rahmani, B. Majdoleslam, I. Abdollahi, S. S. Ali, and A. Ahmad, "Reliability of Surface Electromyography in the Assessment of Paraspinal Muscle Fatigue: An Updated Systematic Review," *Journal of Manipulative & Physiological Therapeutics*, vol. 37, no. 7, pp. 510–521, Sep. 2014, publisher: Elsevier. [Online]. Available: https://www.jmptonline.org/article/S0161-4754(14)00120-1/fulltext

[40] E. Stålberg and H. van Dijk, "Neurophysiological basis of electromyography," *Muscle Nerve*, vol. 42, no. 4, pp. 515–531, 2010.

[41] M. Al-Ayyad, H. A. Owida, R. De Fazio, B. Al-Naami, and P. Visconti, "Electromyography Monitoring Systems in Rehabilitation: A Review of Clinical Applications, Wearable Devices and Signal Acquisition Methodologies," *Electronics*, vol. 12, no. 7, p. 1520, Jan. 2023, number: 7 Publisher: Multidisciplinary Digital Publishing Institute. [Online]. Available: https://www.mdpi.com/2079-9292/12/7/1520

[42] N. C. Chesler and W. K. Durfee, "Surface EMG as a fatigue indicator during FES-induced isometric muscle contractions," *Journal of Electromyography and Kinesiology*, vol. 7, no. 1, pp. 27–37, Mar. 1997. [Online]. Available: https://www.sciencedirect.com/science/article/pii/S1050641196000168

[43] Y. Liu, H. Yokoi, M. Sugi, and Y. Jiang, "An adaptive filter for surface EMG measurement during FES," in *2024 IEEE International Conference on Cyborg and Bionic Systems (CBS)*, Nov. 2024, pp. 218–222. [Online]. Available: https://ieeexplore.ieee.org/document/10860630

[44] M. O. Ibitoye, E. H. Estigoni, N. A. Hamzaid, A. K. A. Wahab, and G. M. Davis, "The Effectiveness of FES-Evoked EMG Potentials to Assess Muscle Force and Fatigue in Individuals with Spinal Cord Injury," *Sensors (Basel, Switzerland)*, vol. 14, no. 7, pp. 12 598–12 622, Jul. 2014. [Online]. Available: https://www.ncbi.nlm.nih.gov/pmc/articles/PMC4168418/

[45] P. Li, X. Yang, G. Yin, and J. Guo, "Skeletal Muscle Fatigue State Evaluation with Ultrasound Image Entropy," *Ultrasonic Imaging*, vol. 42, no. 6, pp. 235–244, Nov. 2020, publisher: SAGE Publications Inc. [Online]. Available: https://doi.org/10.1177/0161734620952683

[46] Q. Zhang, A. Iyer, K. Lambeth, K. Kim, and N. Sharma, "Ultrasound Echogenicity-based Assessment of Muscle Fatigue During Functional Electrical Stimulation," in *2021 43rd Annual International Conference of the IEEE Engineering in Medicine & Biology Society (EMBC)*, Nov. 2021, pp. 5948–5952, iSSN: 2694-0604. [Online]. Available: https://ieeexplore.ieee.org/abstract/document/9630325

[47] J. Shi, Z. Yan, L. Xue, and Y. Zheng, "Evaluation of the Muscle Fatigue Based on Ultrasound Images," in *2006 6th World Congress on Intelligent Control and Automation*, vol. 2, Jun. 2006, pp. 10 332–10 336. [Online]. Available: https://ieeexplore.ieee.org/document/1714026

[48] J. P. Williams, R. Nathanson, C. M. LoPresti, M. J. Mader, E. K. Haro, B. Drum, E. O'Brien, R. Khosla, J. S. Boyd, B. Bales, E. Wetherbee, H. Sauthoff, C. K. Schott, Z. Basrai, D. Resop, B. P. Lucas, and N. J. Soni, "Current use, training, and barriers in point-of-care ultrasound in hospital medicine: A national survey of VA hospitals," *Journal of Hospital Medicine*, vol. 17, no. 8, pp. 601–608, 2022, _eprint: https://shmpublications.onlinelibrary.wiley.com/doi/pdf/10.1002/jhm.12911. [Online]. Available: https://onlinelibrary.wiley.com/doi/abs/10.1002/jhm.12911

[49] C. Giangrossi, A. Ramalli, A. Dallai, D. Mazierli, V. Meacci, E. Boni, and P. Tortoli, "Requirements and Hardware Limitations of High-Frame-Rate 3-D Ultrasound Imaging Systems," *Applied Sciences*, vol. 12, no. 13, p. 6562, Jan. 2022, number: 13 Publisher: Multidisciplinary Digital Publishing Institute. [Online]. Available: https://www.mdpi.com/2076-3417/12/13/6562

[50] Q. Zhang, A. Iyer, K. Lambeth, K. Kim, and N. Sharma, "Ultrasound Echogenicity as an Indicator of Muscle Fatigue during Functional Electrical Stimulation," *Sensors (Basel, Switzerland)*, vol. 22, no. 1, p. 335, Jan. 2022. [Online]. Available: https://www.ncbi.nlm.nih.gov/pmc/articles/PMC8749646/

[51] M. A. Islam, K. Sundaraj, R. B. Ahmad, and N. U. Ahamed, "Mechanomyogram for Muscle Function Assessment: A Review," *PLOS ONE*, vol. 8, no. 3, p. e58902, Mar. 2013, publisher: Public Library of Science. [Online]. Available: https://journals.plos.org/plosone/article?id=10.1371/journal.pone.0058902

[52] M. O. Ibitoye, N. A. Hamzaid, J. M. Zuniga, N. Hasnan, and A. K. A. Wahab, "Mechanomyographic Parameter Extraction Methods: An Appraisal for Clinical

Applications," *Sensors (Basel, Switzerland)*, vol. 14, no. 12, pp. 22 940–22 970, Dec. 2014. [Online]. Available: https://www.ncbi.nlm.nih.gov/pmc/articles/PMC4299047/

[53] M. T. Tarata, "Mechanomyography versus Electromyography, in monitoring the muscular fatigue," *BioMedical Engineering OnLine*, vol. 2, no. 1, p. 3, Feb. 2003. [Online]. Available: https://doi.org/10.1186/1475-925X-2-3

[54] T. W. Beck, T. J. Housh, G. O. Johnson, J. P. Weir, J. T. Cramer, J. W. Coburn, and M. H. Malek, "Mechanomyographic and electromyographic time and frequency domain responses during submaximal to maximal isokinetic muscle actions of the biceps brachii," *European Journal of Applied Physiology*, vol. 92, no. 3, pp. 352–359, Jul. 2004. [Online]. Available: https://doi.org/10.1007/s00421-004-1110-9

[55] R. Uwamahoro, K. Sundaraj, and I. D. Subramaniam, "Assessment of muscle activity using electrical stimulation and mechanomyography: a systematic review," *BioMedical Engineering OnLine*, vol. 20, no. 1, p. 1, Jan. 2021. [Online]. Available: https://doi.org/10.1186/s12938-020-00840-w

[56] E. Krueger, L. Popović-Maneski, and P. Nohama, "Mechanomyography-Based Wearable Monitor of Quasi-Isometric Muscle Fatigue for Motor Neural Prostheses," *Artificial Organs*, vol. 42, no. 2, pp. 208–218, Feb. 2018.

[57] I. Talib, K. Sundaraj, and C. K. Lam, "Choice of Mechanomyography Sensors for Diverse Types of Muscle Activities," *Journal of Telecommunication, Electronic and Computer Engineering (JTEC)*, vol. 10, no. 1-13, pp. 79–82, May 2018, number: 1-13. [Online]. Available: https://jtec.utem.edu.my/jtec/article/view/4125

[58] S. Ahn, I. Shin, and Y. Kim, "The effect of accelerometer mass in mechanomyography measurements," *Journal of Vibroengineering*, vol. 18, no. 7, pp. 4736–4742, Nov. 2016, number: 7 Publisher: JVE International Ltd. [Online]. Available: https://www.extrica.com/article/17420

[59] A. Courteville, T. Gharbi, and J. Cornu, "MMG measurement: a high-sensitivity microphone-based sensor for clinical use," *IEEE Transactions on Biomedical Engineering*, vol. 45, no. 2, pp. 145–150, Feb. 1998. [Online]. Available: https://ieeexplore.ieee.org/document/661262

[60] M. Watakabe, K. Mita, K. Akataki, and Y. Itoh, "Mechanical behaviour of condenser microphone in mechanomyography," *Medical and Biological Engineering and Computing*, vol. 39, no. 2, pp. 195–201, Mar. 2001. [Online]. Available: https://doi.org/10.1007/BF02344804

[61] M. Watakabe, Y. Itoh, K. Mita, and K. Akataki, "Technical aspects of mechnomyography recording with piezoelectric contact sensor," *Medical & Biological Engineering & Computing*, vol. 36, no. 5, pp. 557–561, Sep. 1998.

[62] "Systematic review on the application of wearable inertial sensors to quantify everyday life motor activity in people with mobility impairments | Journal of NeuroEngineering and Rehabilitation | Full Text." [Online]. Available: https://jneuroengrehab.biomedcentral.com/articles/10.1186/s12984-020-00779-y?utm_source=chatgpt.com

[63] G. Ciuti, L. Ricotti, A. Menciassi, and P. Dario, "MEMS Sensor Technologies for Human Centred Applications in Healthcare, Physical Activities, Safety and Environmental Sensing: A Review on Research Activities in Italy," *Sensors (Basel, Switzerland)*, vol. 15, no. 3, pp. 6441–6468, Mar. 2015. [Online]. Available: https://www.ncbi.nlm.nih.gov/pmc/articles/PMC4435109/

[64] A. O. Posatskiy and T. Chau, "The effects of motion artifact on mechanomyography: A comparative study of microphones and accelerometers," *Journal of Electromyography and Kinesiology*, vol. 22, no. 2, pp. 320–324, Apr. 2012. [Online]. Available: https://www.sciencedirect.com/science/article/pii/S1050641111001441

[65] C. Orizio, "Muscle sound: bases for the introduction of a mechanomyographic signal in muscle studies," *Critical Reviews in Biomedical Engineering*, vol. 21, no. 3, pp. 201–243, 1993.

[66] K. Mishra, S. Basyal, J. Ting, and B. C. Allen, "Arise control of an uncertain lower-limb hybrid exoskeleton," in *2025 International Conference On Rehabilitation Robotics (ICORR)*. IEEE, 2025, pp. 1–6.

[67] A. J. C. McMorland, K. D. Runnalls, and W. D. Byblow, "A Neuroanatomical Framework for Upper Limb Synergies after Stroke," *Frontiers in Human Neuroscience*, vol. 9, Feb. 2015, publisher: Frontiers. [Online]. Available: https://www.frontiersin.org/journals/human-neuroscience/articles/10.3389/fnhum.2015.00082/full

[68] D. J. Oranchuk, A. G. Storey, A. R. Nelson, and J. B. Cronin, "Isometric training and long-term adaptations: Effects of muscle length, intensity, and intent: A systematic review," *Scandinavian Journal of Medicine & Science in Sports*, vol. 29, no. 4, pp. 484–503, 2019, _eprint: https://onlinelibrary.wiley.com/doi/pdf/10.1111/sms.13375. [Online]. Available: https://onlinelibrary.wiley.com/doi/abs/10.1111/sms.13375

[69] M. J. Wiest, A. J. Bergquist, M. G. Heffernan, M. Popovic, and K. Masani, "Fatigue and Discomfort During Spatially Distributed Sequential Stimulation of Tibialis Anterior," *IEEE Transactions on Neural Systems and Rehabilitation Engineering*, vol. 27, no. 8, pp. 1566–1573, Aug. 2019. [Online]. Available: https://ieeexplore.ieee.org/document/8752432/

[70] T. Schauer, "Sensing motion and muscle activity for feedback control of functional electrical stimulation: Ten years of experience in Berlin," *Annual Reviews in Control*, vol. 44, pp. 355–374, Jan. 2017. [Online]. Available: https://www.sciencedirect.com/science/article/pii/S1367578817301141

[71] K. Akataki, K. Mita, M. Watakabe, and K. Itoh, "Mechanomyogram and force relationship during voluntary isometric ramp contractions of the biceps brachii muscle," *European Journal of Applied Physiology*, vol. 84, no. 1-2, pp. 19–25, 2001.

[72] D. Lum and T. M. Barbosa, "Brief Review: Effects of Isometric Strength Training on Strength and Dynamic Performance," *International Journal of Sports Medicine*, vol. 40,

pp. 363–375, Apr. 2019, publisher: © Georg Thieme Verlag KG. [Online]. Available: https://www.thieme-connect.de/products/ejournals/abstract/10.1055/a-0863-4539

[73] I. Talib, K. Sundaraj, and C. K. Lam, "Analysis of the crosstalk in mechanomyographic signals along the longitudinal, lateral and transverse axes of elbow flexor muscles during sustained isometric forearm flexion, supination and pronation exercises," *Journal of Musculoskeletal & Neuronal Interactions*, vol. 20, no. 2, pp. 194–205, 2020. [Online]. Available: https://www.ncbi.nlm.nih.gov/pmc/articles/PMC7288391/

[74] F. Zaheer, S. H. Roy, and C. J. De Luca, "Preferred Sensor Sites for Surface EMG Signal Decomposition," *Physiological measurement*, vol. 33, no. 2, pp. 195–206, Feb. 2012. [Online]. Available: https://www.ncbi.nlm.nih.gov/pmc/articles/PMC3428954/

[75] E. Krueger, E. M. Scheeren, G. N. Nogueira-Neto, V. L. D. S. N. Button, and P. Nohama, "Advances and perspectives of mechanomyography," *Revista Brasileira de Engenharia Biomédica*, vol. 30, no. 4, pp. 384–401, Dec. 2014. [Online]. Available: http://www.scielo.br/scielo.php?script=sci_arttext&pid=S1517-31512014000400009&lng=en&tlng=en

[76] C. Orizio, M. Gobbo, B. Diemont, F. Esposito, and A. Veicsteinas, "The surface mechanomyogram as a tool to describe the influence of fatigue on biceps brachii motor unit activation strategy. Historical basis and novel evidence," *European Journal of Applied Physiology*, vol. 90, no. 3, pp. 326–336, Oct. 2003. [Online]. Available: https://doi.org/10.1007/s00421-003-0924-1

[77] M. Shinohara and K. Søgaard, "Mechanomyography for Studying Force Fluctuations and Muscle Fatigue," *Exercise and Sport Sciences Reviews*, vol. 34, no. 2, p. 59, Apr. 2006. [Online]. Available: https://journals.lww.com/acsm-essr/fulltext/2006/04000/Mechanomyography_for_Studying_Force_Fluctuations.4.aspx

[78] S. B. Rodrigues, L. P. de Faria, A. M. Monteiro, J. L. Lima, T. M. Barbosa, and J. A. Duarte, "EMG Signal Processing for the Study of Localized Muscle Fatigue—Pilot Study to Explore the Applicability of a Novel Method," *International Journal of*

Environmental Research and Public Health, vol. 19, no. 20, p. 13270, Jan. 2022, number: 20 Publisher: Multidisciplinary Digital Publishing Institute. [Online]. Available: https://www.mdpi.com/1660-4601/19/20/13270

[79] T. W. Beck, T. J. Housh, J. T. Cramer, J. P. Weir, G. O. Johnson, J. W. Coburn, M. H. Malek, and M. Mielke, "Mechanomyographic amplitude and frequency responses during dynamic muscle actions: a comprehensive review," *BioMedical Engineering OnLine*, vol. 4, no. 1, p. 67, Dec. 2005. [Online]. Available: https://doi.org/10.1186/1475-925X-4-67

[80] W. Jiang, C. Xia, Y. Zhang, J. Xie, and W. Feng, "Research on Muscle Fatigue Trend via Nonlinear Dynamic Feature Analysis of Mechanomyography Signal," in *2019 IEEE 4th International Conference on Signal and Image Processing (ICSIP)*, Jul. 2019, pp. 669–673.

[81] M. A. Dzulkifli, N. A. Hamzaid, G. M. Davis, and N. Hasnan, "Neural Network-Based Muscle Torque Estimation Using Mechanomyography During Electrically-Evoked Knee Extension and Standing in Spinal Cord Injury," *Frontiers in Neurorobotics*, vol. 12, Aug. 2018, publisher: Frontiers. [Online]. Available: https://www.frontiersin.orghttps://www.frontiersin.org/journals/neurorobotics/articles/10.3389/fnbot.2018.00050/full

[82] T. W. Beck, V. von Tscharner, T. J. Housh, J. T. Cramer, J. P. Weir, M. H. Malek, and M. Mielke, "Time/frequency events of surface mechanomyographic signals resolved by nonlinearly scaled wavelets," *Biomedical Signal Processing and Control*, vol. 3, no. 3, pp. 255–266, Jul. 2008. [Online]. Available: https://www.sciencedirect.com/science/article/pii/S1746809408000153

[83] B. J. Schoenfeld, J. Grgic, D. W. Van Every, and D. L. Plotkin, "Loading Recommendations for Muscle Strength, Hypertrophy, and Local Endurance: A Re-Examination of the Repetition Continuum," *Sports*, vol. 9, no. 2, p. 32, Feb. 2021. [Online]. Available: https://www.ncbi.nlm.nih.gov/pmc/articles/PMC7927075/

[84] Y. Yoshitake, H. Ue, M. Miyazaki, and T. Moritani, “Assessment of lower-back muscle fatigue using electromyography, mechanomyography, and near-infrared spectroscopy,” *European Journal of Applied Physiology*, vol. 84, no. 3, pp. 174–179, Mar. 2001. [Online]. Available: https://doi.org/10.1007/s004210170001

[85] E. C. Hill, “Electromyographic and Mechanomyographic Time and Frequency Responses During Fatiguing, Submaximal, Isokinetic Muscle Actions of the Biceps Brachii.”

[86] J. S. Gomes, J. H. Oliveira, P. Bauer, P. Pezarat-Correia, and J. R. Vaz, “Changes in torque complexity with fatigue are related to motor unit behaviour,” *Scientific Reports*, vol. 15, no. 1, Apr. 2025, publisher: Springer Science and Business Media LLC. [Online]. Available: https://www.nature.com/articles/s41598-025-96102-7

[87] R. B. Woodward, M. J. Stokes, S. J. Shefelbine, and R. Vaidyanathan, “Segmenting Mechanomyography Measures of Muscle Activity Phases Using Inertial Data,” *Scientific Reports*, vol. 9, no. 1, p. 5569, Apr. 2019, publisher: Nature Publishing Group. [Online]. Available: https://www.nature.com/articles/s41598-019-41860-4

[88] S. E. I. E. N. U. M. E. Z. Davis W. Poole, Paxton C. Albright and C. G. Rose, “Design and validation of caset: A lift-assistance supernumerary finger,” *Ergonomics*, pp. 1–17, 2025, in review.

[89] A. Finneran and L. O’Sullivan, “Effects of grip type and wrist posture on forearm EMG activity, endurance time and movement accuracy,” *International Journal of Industrial Ergonomics*, vol. 43, no. 1, pp. 91–99, Jan. 2013. [Online]. Available: https://www.sciencedirect.com/science/article/pii/S0169814112001199

[90] T. Konno and K. Watanabe, “Morpho-functional relationship between muscular architecture and proportion of myofiber types in ovine antebrachial musculature,” *Okajimas Folia Anatomica Japonica*, vol. 89, no. 2, pp. 51–56, 2012, publisher: Department of Anatomy Keio University School of Medicine. [Online]. Available: http://jlc.jst.go.jp/DN/JST.JSTAGE/ofaj/89.51?lang=en&from=CrossRef&type=abstract

[91] D. H. Rosero-Salazar, "Image Analysis of Oxidative and Glycolytic Muscle Fibers During Reperfusion Injury by Segmentation Based on Regions," *International Journal of Morphology*, vol. 34, no. 1, pp. 127–135, Mar. 2016, publisher: SciELO Agencia Nacional de Investigacion y Desarrollo (ANID). [Online]. Available: http://www.scielo.cl/scielo.php?script=sci_arttext&pid=S0717-95022016000100019&lng=en&nrm=iso&tlng=en

[92] N. K. Mamaghani, Y. Shimomura, K. Iwanaga, and T. Katsuura, "Mechanomyogram and Electromyogram Responses of Upper Limb During Sustained Isometric Fatigue with Varying Shoulder and Elbow Postures." *Journal of PHYSIOLOGICAL ANTHROPOLOGY and Applied Human Science*, vol. 21, no. 1, pp. 29–43, 2002. [Online]. Available: http://www.jstage.jst.go.jp/article/jpa/21/1/21_1_29/_article

[93] A. Adam, C. J. De Luca, and Z. Erim, "Hand dominance and motor unit firing behavior," *Journal of Neurophysiology*, vol. 80, no. 3, pp. 1373–1382, Sep. 1998.

[94] M. Hribernik, A. Umek, S. Tomažič, and A. Kos, "Review of Real-Time Biomechanical Feedback Systems in Sport and Rehabilitation," *Sensors*, vol. 22, no. 8, p. 3006, Jan. 2022, number: 8 Publisher: Multidisciplinary Digital Publishing Institute. [Online]. Available: https://www.mdpi.com/1424-8220/22/8/3006

[95] A. Christou, A. J. Del-Ama, J. C. Moreno, and S. Vijayakumar, "Adaptive Control for Triadic Human-Robot-FES Collaboration in Gait Rehabilitation: A Pilot Study," in *2024 IEEE International Conference on Robotics and Automation (ICRA)*, May 2024, pp. 5561–5568. [Online]. Available: https://ieeexplore.ieee.org/document/10611133